

Search for Isobaric Analogue States in ^{57}Co Via The Reaction $^{56}\text{Fe}(\rho,\gamma)^{57}\text{Co}$

by

Muhammad Ahmad Garwan

A Thesis Presented to the

FACULTY OF THE COLLEGE OF GRADUATE STUDIES

KING FAHD UNIVERSITY OF PETROLEUM & MINERALS

DHAHRAN, SAUDI ARABIA

In Partial Fulfillment of the
Requirements for the Degree of

MASTER OF SCIENCE

In

NUCLEAR PHYSICS

May, 1985

INFORMATION TO USERS

This manuscript has been reproduced from the microfilm master. UMI films the text directly from the original or copy submitted. Thus, some thesis and dissertation copies are in typewriter face, while others may be from any type of computer printer.

The quality of this reproduction is dependent upon the quality of the copy submitted. Broken or indistinct print, colored or poor quality illustrations and photographs, print bleedthrough, substandard margins, and improper alignment can adversely affect reproduction.

In the unlikely event that the author did not send UMI a complete manuscript and there are missing pages, these will be noted. Also, if unauthorized copyright material had to be removed, a note will indicate the deletion.

Oversize materials (e.g., maps, drawings, charts) are reproduced by sectioning the original, beginning at the upper left-hand corner and continuing from left to right in equal sections with small overlaps. Each original is also photographed in one exposure and is included in reduced form at the back of the book.

Photographs included in the original manuscript have been reproduced xerographically in this copy. Higher quality 6" x 9" black and white photographic prints are available for any photographs or illustrations appearing in this copy for an additional charge. Contact UMI directly to order.

U·M·I

University Microfilms International
A Bell & Howell Information Company
300 North Zeeb Road, Ann Arbor, MI 48106-1346 USA
313/761-4700 800/521-0600

Order Number 1355748

**Search for isobaric analogue states in ^{57}Co via the reaction ^{56}Fe
(p, γ) ^{57}Co**

Garwan, Muhammad Ahmad, M.S.

King Fahd University of Petroleum and Minerals (Saudi Arabia), 1985

U·M·I

**300 N. Zeeb Rd.
Ann Arbor, MI 48106**

University of Petroleum and Minerals

SEARCH FOR ISOBARIC ANALOGUE STATES IN

^{57}Co VIA THE REACTION $^{56}\text{Fe} (p, \gamma) ^{57}\text{Co}$

BY

MUHAMMAD AHMAD GARWAN

A Thesis Presented to the
FACULTY OF THE COLLEGE OF GRADUATE STUDIES

In Partial Fulfillment of the
Requirements for the Degree of
The Library

University of Petroleum & Minerals
Dhahran, Saudi Arabia

MASTER OF SCIENCE
IN

NUCLEAR PHYSICS

MAY 1985

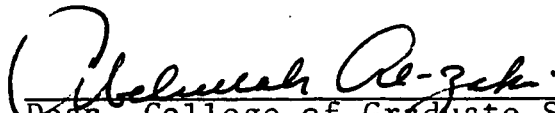
UNIVERSITY OF PETROLEUM AND MINERALS

DHAHRAN, SAUDI ARABIA

COLLEGE OF GRADUATE STUDIES

This thesis, written by MR. MUHAMMAD AHMAD GARWAN under the direction of his Thesis Committee and approved by all its members has been presented to and accepted by the Dean, College of Graduate Studies, in partial fulfilment of the requirements for the degree of Master of Science in Nuclear Physics.

SPEC
A
1
G 37
C. 2


Dean, College of Graduate Studies


Date : 9-3-1985


Department Chairman

616066 - 616241

Thesis Committee


Dr. M.S. El-Kateb (Chairman)


Dr. A.H. Hussein (Member)


Dr. A.K. Abdallah (Member)

بِسْمِ اللَّهِ
الرَّحْمَنِ
الرَّحِيمِ

ABSTRACT

The $^{56}\text{Fe}(\text{p},\gamma)^{57}\text{Co}$ reaction has been studied over the proton energy range of $E_{\text{p}}=3694\text{--}3855$ keV. Four resonances were observed at $E_{\text{p}}=3720$, 3727, 3774 and 3793 keV. Decay schemes were established for the four resonances, and angular distributions were measured at $E_{\text{p}}=3720$, 3774 and 3793 keV. A $J^{\pi}=9/2^{+}$ has been assigned for the resonances at $E_{\text{p}}=3720$ and 3727 keV, and $J^{\pi}=5/2^{+}$ has been assigned for the resonances at $E_{\text{p}}=3774$ and 3793 keV.

In this work it was concluded that the two resonances at $E_{\text{p}}=3720$ and 3727 keV ($E_{\text{x}}=9682$ and 9689 keV) are fragments of an isobaric analogue state in ^{57}Co corresponding to the $g_{9/2}$ at $E_{\text{x}}=2455$ keV in ^{57}Fe . Moreover, it was concluded that the two resonances at $E_{\text{p}}=3774$ and 3793 keV ($E_{\text{x}}=9734$ and 9753 keV) are two fragments of an isobaric analogue state in ^{57}Co corresponding to the $d_{5/2}$ at $E_{\text{x}}=2506$ keV in ^{57}Fe .

Levels at $E_{\text{x}}=4586$ and 4675 keV in ^{57}Co are identified as the antianalogue states (T^{\leq}) corresponding to the $g_{9/2}$ and $d_{5/2}$ isobaric analogue states respectively.

الخلاصة

في هذا البحث دُرِسَ التفاعل النووي الناتج عن تسليط شعاع مـــــــن البروتونات بطاقة تدريجية من ٣٦٩٤ حتى ٣٨٥٥ ألف إلكترون فولت ، على ذرات عنصر الحديد ٥٦ لتتكون بذلك نُوى مركبة للكوبلت ٥٧ في حالات مُشكّاة مختلفة الطاقة . وبدراسة أطياف أشعة جاما الصادرة عن التفاعل تم تحديد أربع حالات رنين عند طاقات البروتونات ٣٧٢٠ ، ٣٧٢٧ ، ٣٧٧٤ و ٣٧٩٣ ألف إلكترون فولت حيث أُشيرت أربع حالات لنواة الكوبلت ٥٧ هي ٩٦٨٢ ، ٩٦٨٩ ، ٩٧٣٤ و ٩٧٥٣ ألف إلكترون فولت على التوالي .

درست هذه الحالات الأربع بِجَمْعٍ أطياف لأشعة جاما الصادرة عن كل حاله ، ثم جُمِعَت قياسات التوزع الزاوي لغزارة أشعة جاما لدى اضمحلال الحالات المُشارَة عند طاقات البروتونات ٣٧٢٠ ، ٣٧٧٤ و ٣٧٩٣ ألف إلكترون فولت .

بعد تحليل القياسات السابقه ، تم حساب نِسَب التفرع لاضمحلال كــــل الحالات الأربع المشارَة في هذه الدراسة ، وتم تحديد قيمة الزخم الزاوي ونوعية التماثل لتلك الحالات أيضًا . فُحِدَّ الزخم الزاوي بـ $\frac{9}{2}$ و تماثل ايجابي للحالتين ٩٦٨٢ و ٩٦٨٩ ألف إلكترون فولت ، و بـ $\frac{5}{2}$ و تماثل ايجابي للحالتين ٩٧٣٤ و ٩٧٥٣ ألف إلكترون فولت .

ونظرا لكون نواة الكوبلت ٥٧ منازرة لنواة الحديد ٥٧ فقد تمَّ التعرُّف على الحالتين ٩٦٨٢ و ٩٦٨٩ ألف إلكترون فولت ككسرتين كلاهما منازرة للحالة ٢٤٥٥ ألف إلكترون فولت من الحديد ٥٧ ذات الزخم الزاوي $\frac{9}{2}$ والايجابية التماثل . أما الحالتين ٩٧٣٤ و ٩٧٥٣ ألف إلكترون فولت فأیضا تمَّ التعرُّف عليهما ككسرتين كلاهما منازرة للمستوى ٢٥٠٦ ألف إلكترون فولت من الحديد ٥٧ ذات الزخم الزاوي $\frac{5}{2}$ والايجابية التماثل . وأخيرا تم تحديد الحالتين ٤٥٨٦ و ٤٦٧٥ ألف إلكترون فولت كنظيرتين سفليتين ، الأولى للحالتين $\frac{9}{2}$ موجبه التماثل والثانية للحالتين $\frac{5}{2}$ موجبة التماثل أيضًا .

ACKNOWLEDGMENTS

I am deeply indebted to the University of Petroleum & Minerals (UPM) for the constant support of this work throughout all stages of its performance.

I am also grateful to Dr. Salah El-Kateb for the endurance and the help he showed as my Thesis Advisor. Thanks are also due to Drs. Darwish Ahmad Darwish, Asad Abdallah and Ahmed Hussein for their encouragement and being members of my thesis committee.

I also thank Drs. George Vourvopoulos and Themis Paradellis for their help and the interest they showed during the experimental measurements of this work.

Comments from the Physics faculty members and help from the Physics Department Chairmen are highly appreciated and my thanks are due to all of them. Thanks are also due to Mr. Mohammad Azam Shad for the excellent job he did in typing this thesis.

Finally, I wish to express my gratitude to all members of my family for their encouragement and understanding.

Table of Contents

Abstract	ii
Abstract (Arabic)	iii
Acknowledgments	iv
Chapter 1 : INTRODUCTION	1
1.1 General	1
1.2 Present Status of the Problem	10
1.3 Present Study	11
Chapter 2 : EXPERIMENTAL AND ANALYTICAL PROCEDURES	14
2.1 Proton Beam	14
2.2 Target and Target Chamber	15
2.3 Detectors and Electronics	17
2.4 Excitation Function and γ -Ray Spectra	18
2.5 Gamma-Ray Angular Distributions	22
Chapter 3 : RESULTS AND DISCUSSION	25
3.1 Excitation Function	25
3.2 Gamma-Ray Spectra & Angular Distributions	25
3.2.1 Resonances at $E_p=3720$ and 3727 keV	25
3.2.2 Resonances at $E_p=3774$ and 3793 keV	29
3.3 Identification of Isobaric Analogue Resonances	31
3.4 Summar and Conclusions	32
Appendix A : Angular Distribution Formalism	60
Appendix B : Selection Rules for γ -Ray Transitions	66
Appendix C : FORTRAN Program	75
References	

LIST OF TABLES

1. Gates of the Excitation Function	20
2. Comparison Between Branching Ratios of the $g_{9/2}$ IAS from Different Works 	54
3. Summary of Angular Distribution Results at $E_p=3720$ keV.	
4. Summary of Angular Distribution Results at $E_p=3774$ keV. 	56
5. Summary of Angular Distribution Results at $E_p=3793$ keV. 	58
6. Comparison Between Expected and Observed IAS	59
7. Possible Multipolarities for γ -Ray Transition	69

LIST OF FIGURES

1. Analogue States in an Isobar	7
2. The ^{57}Fe - ^{57}Co Isobar	13
3. Target Chamber and Detectors	16
4. Detectors and Electronics Block Diagram	19
5. Excitation Function	35
6. Gamma-Ray Spectra at $E_p=3720, 3727$ and 3712 keV	36
7. The Decay Scheme for Resonances at $E_p=3720$ & 3727 keV	37
8. Experimental Angular Distribution Data and Its Least Squares Fits for $E_p=3720$ keV	38
9. Qui-Squares Fits for $9682 \rightarrow \text{G.S.}$	39
10. Qui-Squares Fits for $9682 \rightarrow 4586$ keV	40
11. Qui-Squares Fits for $9682 \rightarrow 2611$ keV	41
12. Gamma-Ray Spectra at $E_p=3774, 3793$ and 3786 keV	42
13. The Decay Scheme for Resonances at $E_p=3774$ & 3793 keV	43
14. Experimental Data and Its Least Squares Fits for $E_p=3774$ keV	44
15. Qui-Squares Fits for $9734 \rightarrow \text{G.S.}$	45
16. Qui-Squares Fits for $9734 \rightarrow 1378$ keV	46
17. Qui-Squares Fits for $9734 \rightarrow 1758$ keV	47
18. Qui-Squares Fits for $9734 \rightarrow 4675$ keV	48
19. Experimental Data and Its Least Squares Fits for $E_p=3793$ keV	49
20. Qui-Squares Fits for $9753 \rightarrow \text{G.S.}$	50
21. Qui-Squares Fits for $9753 \rightarrow 1897$ keV	51
22. Qui-Squares Fits for $9753 \rightarrow 4675$ keV	52
23. Summary of all Decay Schemes and Spin Assignments Studied	53
24. Double γ -Ray Cascade	61
25. Symbols for γ -Ray Transition	67

CHAPTER I

INTRODUCTION

1.1. General:

The major breakthrough in nuclear physics was brought about by the work of the British physicist James Chadwick (1) in the Cavendish Laboratory, where he discovered that when beryllium was bombarded by α -particles, it released an unknown chargeless deep penetrating radiation which is capable of ejecting protons from other nuclei. Chadwick published his work in February 1932 describing the new chargeless particle for which he gave the "neutron" as a name. Later, Chadwick (2) was able to find that the mass of the neutron is only slightly larger than that of the proton. It was then concluded that nuclei consist only of protons and neutrons, with both of them to be regarded as the fundamental constituents of the nucleus (3,4). The discovery of neutron paved the way for the study of the forces within the nucleus of the deuteron (5,6). Another subatomic particle, the positron (7) was postulated by Dirac (8) in 1930 and then experimentally reported by C.D. Anderson (9) in 1932. The discovery of the positron made possible for physicists to neatly explain the mechanism of β -decay (10).

The year 1932 also gave birth to the first particle accelerator, which was the voltage multiplier of Cockcroft and Walton (11). Later on also Van De Graaff introduced his electrostatic generator (12), and by the year 1936 the Cyclotron of Lawrence and Livingston was able to accelerate protons, deuterons and α -particles to energies as high as several millions of electron volts.

The idea of charge symmetry was postulated by Heisenberg in his first paper on the proton-neutron model of the nucleus (13). He considered the forces acting between pairs of neutrons to be almost equal to those between pairs of protons. He also concluded that the variation of charge mass ratios of stable elements through the periodic table was due to the electrostatic repulsion between protons. In light nuclei where electrostatic forces are less pronounced the ratio N/Z is almost one. The charge symmetry hypothesis meant that all non-electrical forces are completely symmetrical between neutrons and protons. Quantitative applications were predicted for charge symmetry and experimental tests for its validity started in 1936 by the study of binding energy differences in mirror nuclei (as we will see later in this chapter). One of the early works on nucleon-nucleon forces was the proton-proton scattering experiment of Tuve et al. (14); as a result of this experiment Breit

et al. (15) were able to show that proton-proton and neutron-neutron interactions are similar when taken over the same energy range. The similarity of non-electrostatic forces between protons to that between a proton and a neutron, together with the charge symmetry principle gave the hypothesis of charge independence : interactions between all pairs of nuclear particles are the same (with the exception of electrostatic forces). The hypothesis of charge independence provided the direct linkage between elementary particle physics and nuclear physics. The conservation laws of isobaric spin and strangeness in elementary particle physics are direct extensions of the symmetry borne in the charge independence hypothesis in nuclear physics. In both classical and quantum physics, symmetry phenomena always imply some conservation laws. In quantum physics new quantum numbers are introduced for every symmetry, where these numbers give the eigenvalues of the conserved quantity. Charge independence and charge symmetry introduced new physical symmetries that should be expressed in new conservation laws and corresponding quantum numbers. In 1937 and 1939 Wigner (16,17) studied the properties of nuclear states implied by charge independence. Selection rules were derived later on by Adair (18) and Kroll et al. (19). Wigner (16,17) used Heisenberg's concept (13) of the neutron and proton as two states of a single particle,

the nucleon, and generalized the charge independence hypothesis into the formalism of isospin (isobaric) spin of nuclei. The isospin formalism is identical to that of physical spin. An abstract vector operator \vec{t} in the abstract isospin spin space is quite analogous to the spin vector operator in physical spin space, and hence an eigenfunction of \vec{t} will have an isospin quantum number which gives the "length" of \vec{t} from the relation:

$$|\vec{t}|^2 = t(t + 1)$$

There are $2t + 1$ eigenfunctions with isospin spin t each has a different value of t_3 , where t_3 is the component of \vec{t} along an abstract direction in space called the charge axis. Treating the proton and the neutron as two charge states of a nucleon means that they both have their isotopic spin equal to $1/2$. The possible values of t_3 now are $\pm 1/2$, and it is arbitrary which of the nucleons takes the positive and which takes the negative. However, in nuclear physics, it is the convention that the neutron state is assigned the positive t_3 and the proton is assigned the negative value of t_3 . The total isospin operator of a system of nucleons \vec{T} , is obtained by vectorially summing up the isospin operators of all the constituents of the system.

$$\vec{T} = \sum_{i=1}^A \vec{t}_i \quad (A \text{ number of nucleons})$$

$$\text{Hence, } T_3 = \sum_{i=1}^A t_{3i} = \frac{N - Z}{2}, \text{ where } N \text{ is the}$$

number of neutrons and Z is the number of protons in a system of A nucleons. The sign convention chosen above makes the values of T_3 to be non-negative for all stable nuclei except ${}^3\text{He}$ and the proton. A strong support for the isotopic spin formalism comes from the experimental measurement of binding energy difference between mirror nuclei. One of the early works in this regard was the investigation of the positron decay of a number of elements having Z protons and $Z-1$ neutrons into the mirror nuclei having $Z-1$ protons and Z neutrons. Fowler et al. (20) bombarded several elements with 1 MeV deuterons. They then measured the maximum energies of the positrons produced in the decay, and used it in determining the difference in binding energy ΔW between the pairs of mirror nuclei. Using several assumptions of which charge symmetry was the main one, they were able to attribute the binding energy difference entirely to electrostatic interaction of the excess charge in the $(Z, Z-1)$ nucleus. However, they supported their findings by classically calculating the electrostatic interaction, and they suggested the formula for binding energy difference as

$$\begin{aligned}\Delta W &= (Z-1) e^2 (r^{-1})_{av} \\ &= \frac{6e^2}{5r_0} (Z-1) A^{-1/3}\end{aligned}$$

where the nuclear radius $R = r_0 A^{1/3}$ and if $r_0 = 1.45$ fm

$$\Delta W = 1.20 (Z-1) A^{-1/3} \text{ MeV}$$

Similar conclusions were arrived at by Bethe (21) about the binding energy difference between ^3H and ^3He . By the year 1941 many more binding energy experiments were performed, and pairs of atomic weights up to 41 had been investigated. Later on better values for the nuclear radius ($r_0=1.2$) were used in the calculations to verify the validity of charge independence (22,23).

With the exclusion of coulomb forces, energies of the excited states as well as the ground states will correspond in the pairs of mirror nuclei. These levels are expected to have the same spin and parity, they are isobaric analogue states (IAS). (See fig.1). In 1949 several research groups started investigating the existence of IAS. The first IAS was reported by Brown et al. (24) in ^7Be via the reaction $^{10}\text{B} (p,\alpha)^7\text{Be}$, the discovered level corresponds to the 479 keV level in ^7Li . The formalism of isobaric spin was applied to light nuclei, and many IAS were identified in doublets

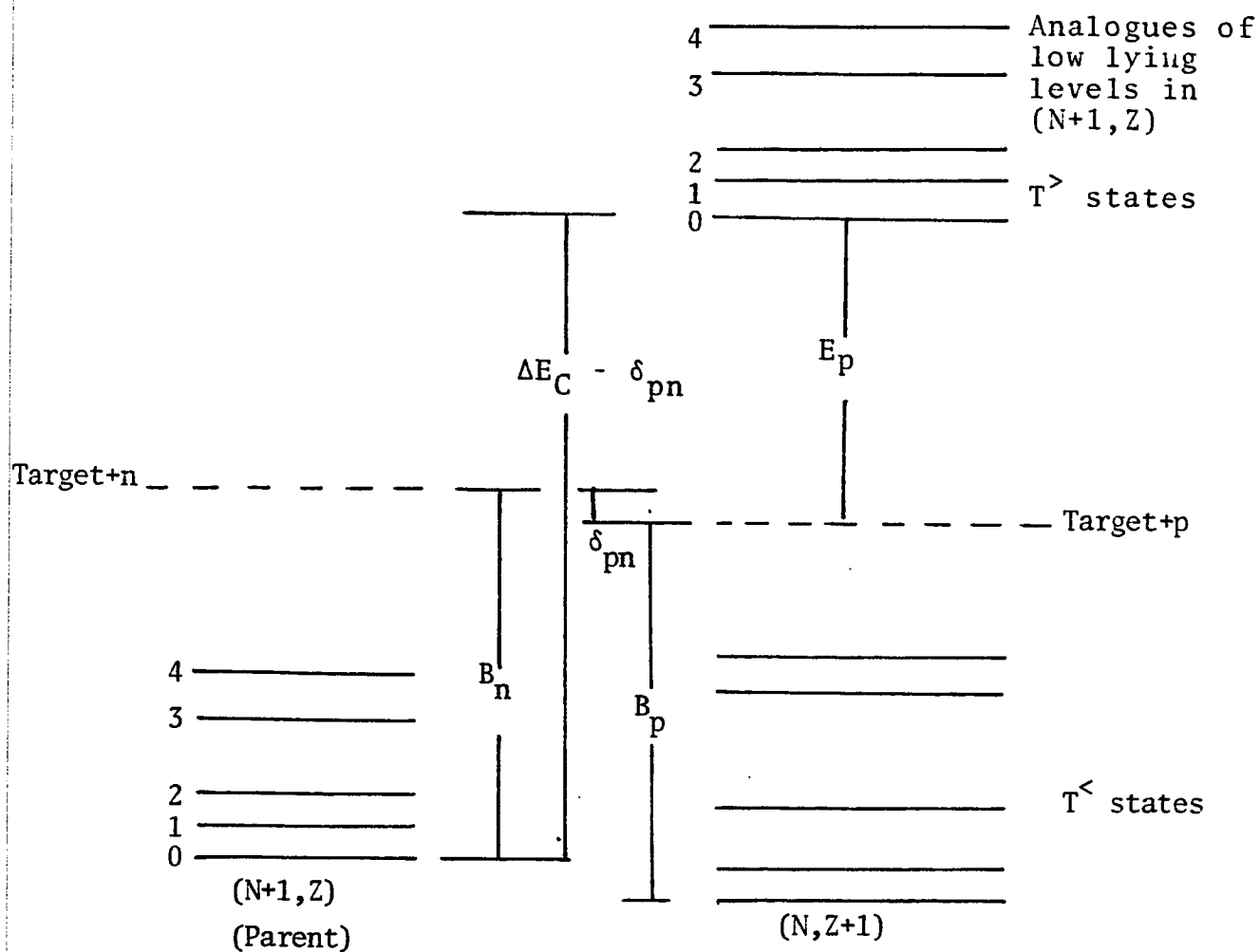


Figure 1 : The coulomb displacement energy relationship between analogue states.

and triplets of nuclei. The identification of IAS in light nuclei was easily accomplished because of their low excitation energies (3-9 MeV/nucleon), low level density and the relatively small coulomb interaction. However, because of the high level density and large coulomb forces in medium and heavy mass nuclei, researchers started to doubt the validity of isobaric spin formalism in that range of nuclei.

Anderson et al. (25-27) studied the $^{51}\text{V} (p,n) ^{51}\text{Cr}$ reaction and concluded that isospin might be a well qualified quantum number over almost all of the nuclei. From that time on many experiments and theoretical studies supported the validity of isospin formalism even in nuclei as heavy as ^{137}Cs (see ref. 28 and references therein).

Resonant scattering of protons, (p,n) charge exchange and (p,γ) radiative capture reactions have provided most of the available data on isobaric analogue resonant states in medium and heavy mass nuclei. The isobaric analogue resonances (IAR) in nuclei were first observed in the (p,n) and proton elastic scattering cross section measurements by a group of Florida State University (28,29). Robson (30) using the quantitative interpretation of Lane (31) pertaining to the (p,n) reaction showed that analogue states could be observed in compound nuclei.

Investigations of analogue resonances in light nuclei (32) via (P, γ) and (P,P) reactions has provided useful information about the characteristics of these resonant states. The initial observations of the gamma-ray decay of analogue states in light nuclei e.g. ^{31}P and ^{35}Cl indicated that electromagnetic transitions had a simple character corresponding to strong M1 between analogue states of given spin and parity ($T^>$) and antianalogue states of the same spin and parity ($T^<$). In addition, these resonances also were observed to have a large reduced proton width and a large γ -ray width (32).

In 1969 and 1970 Maripuu (33-35) concluded that such strong M1 transition between analogue and antianalogue states was a very special case which showed up clearly in light nuclei i.e. in the 2s-1d shell nuclei. Maripuu (33) first noted that strong M1 transitions from analogue to anti-analogue states were confined to single particle states with $J = \ell + \frac{1}{2}$ while those between states with $J = \ell - \frac{1}{2}$ were reduced in strength. Maripuu (34,35) also noted that excitations of states with mixed character (small single particle strength) would not be strongly excited by (P, γ) reactions and when excited would have significantly reduced M1 strengths. The reduction of such M1 strength was explained as a result of the core polarization in the wave function describing the state. The $g_{9/2}$ analogue resonances have been investigated using (P, γ)

reactions on several 1f-2p shell medium mass (even-even and odd-even) target nuclei (36,37). In these nuclei the M1 strength in the $g_{9/2}$ analogue-antianalogue transitions reaches a maximum in the middle of the shell and tends to fall off on either side (38). Such reduction of M1 strength has been qualitatively interpreted as a result of core polarization as well as mixing between $T^>$ and $T^<$ states.

1.2 *Present Status of the Problem:*

The theoretical interest in the study of Cobalt isotopes is implied by their location in the vicinity of the doubly magic ^{56}Ni , they have one proton in the $1f_{7/2}$ subshell and along the series of the cobalt isotopes the $1f_{7/2}$ neutron has its closure (39). Shell model and other theoretical calculations were performed for the cobalt and many other isotopes in the same range of mass number (40-43).

The levels of ^{57}Fe and ^{57}Co have been investigated experimentally by several research groups via variety of reactions (44,45).

Isobaric analogue states in ^{57}Co corresponding to levels up to $E = 1725$ keV state in the ^{57}Fe parent nucleus have been identified via (P,γ) , (P,P) and $(^3\text{He},d)$ reactions

(46-55). The M1 strength for the observed analogue resonances in ^{57}Co were strongly reduced compared to the 2S-1d shell nuclei. Such reduction was interpreted as a result of core polarization effects (54-55).

Recently the decay of the $g_{9/2}$ IAR in ^{57}Co has been investigated through a (P,γ) reaction by two different groups (Fodor et al. (56) and Rangacharyulu et al. (57)). Both groups have examined independently the energy region where the $g_{9/2}$ analogue states in ^{57}Co are expected. However, both groups disagreed on the number of $g_{9/2}$ fragments. In a high resolution experiment, Watson et al. (58) using (P,P) , (P,P^{\sim}) and $(P,P^{\sim}\gamma)$ reactions on ^{56}Fe target identified five $g_{9/2}$ fragments at $E_p = 3698, 3704, 3718, 3731$ and 3751 keV. In another high resolution experiment, Arai et al. (59) using ^{56}Fe (P,P_0) reaction observed only one $g_{9/2}$ resonance at $E_p = 3732$ keV. The $d_{5/2}$ IAR fine structure has been investigated recently via (P,P) , (P,P^{\sim}) and $(P,P^{\sim}\gamma)$ on ^{56}Fe by Watson et al. (58) and ^{56}Fe (P,P_0) reaction by Arai et al. (59).

1.3 Present Study:

In spite of the marked interest in studying the characteristics and systematics of analogue resonances in medium mass nuclei, one can see that in the case of ^{57}Co

nucleus some of these characteristics and systematics have not been established. Moreover, because of the difficulties in identifying the number of $g_{9/2}$ IAR fragments in ^{57}Co through (P,γ) earlier experiments, another investigation appeared necessary to obtain more definitive information regarding the $g_{9/2}$ IAR in ^{57}Co via $^{56}\text{Fe}(\text{P},\gamma)$ reaction. Furthermore, new information is presented in this thesis regarding the $d_{5/2}$ IAR.

The work presented in this thesis was accomplished by measuring the excitation function of the $^{56}\text{Fe}(\text{P},\gamma)$ and $^{56}\text{Fe}(\text{P},\text{P}'\gamma)$ reactions in the $E_p = 3694 - 3855$ keV range. This proton energy range is where one expects the excitation of the $g_{9/2}$ and $d_{5/2}$ IAR (fig.2). Gamma-ray spectra were measured at the $E_p = 3720, 3727, 3774$ and 3793 keV resonances and γ -ray angular distributions were taken at $E_p = 3720, 3774$ and 3793 keV resonances.

The experimental apparatus used to carry out this work along with the procedures followed in the data collection and analysis are presented in Chapter 2. The experimental results, their interpretation as well as the important conclusions which may be drawn from the analysis are presented in Chapter 3.

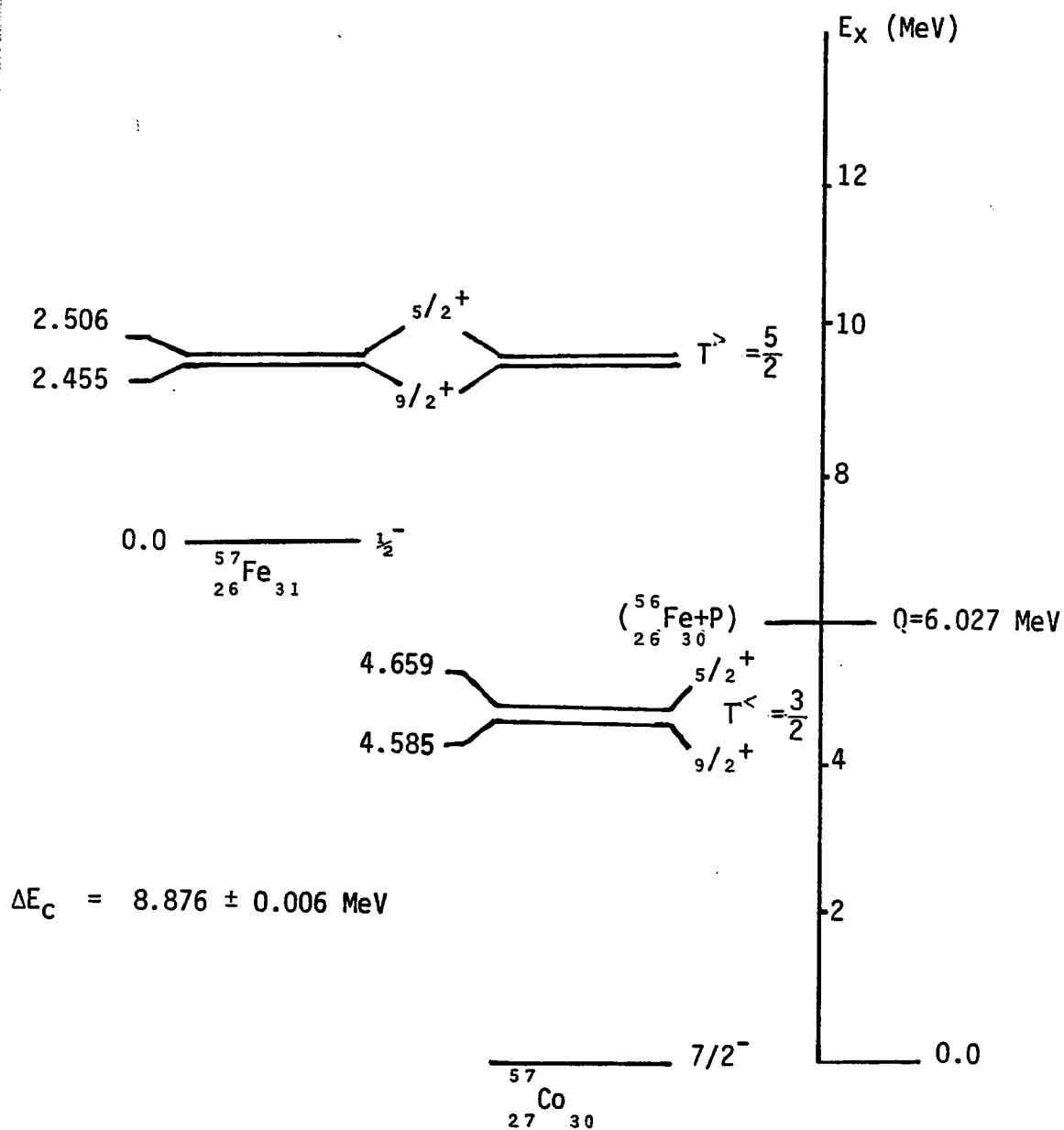


Figure 2. Correspondence between the isobaric analogue states and the levels of ^{57}Fe . This figure indicates the approximate excitation energy at which the $\frac{9}{2}^+$ and the $\frac{5}{2}^+$ resonances are expected.

CHAPTER 2

EXPERIMENTAL AND ANALYTICAL PROCEDURES

2.1 Proton Beam:

The $^{56}\text{Fe} (P,\gamma) ^{57}\text{Co}$ reaction was studied using proton beam from the 5.5 MV $T_{11/25}$ Tandem Van de Graaff accelerator at the Nuclear Research Center, Demokritos, Athens, Greece. An analyzing magnet is used to deflect the vertical ion beam produced by the accelerator into the horizontal direction. The feedback signal about irregularities in the ion beam is produced by a slit system situated near the exit of the analyzing magnet. Feedback signals are fed to the corona probe where they regulate and correct the accelerator terminal voltage. The overall system was capable of keeping the energy of the analyzed protons constant to within ± 750 eV. In defining the shape and size of the beam, two tantalum apertures were used, both were 1.5 mm in diameter and they were located 40 and 90 cm away from the target chamber.

To minimize the difficulties arising from detector dead time, the beam current was kept between 1 and 3 microamperes, depending on the reaction yield at different values of proton energy. The exact beam energy was

determined by precise determination of the magnetic field necessary to bend the proton beam through the 90° analyzing magnet using a nuclear magnetic resonance (NMR) fluxmeter. The absolute value of the calibration constant for the NMR was checked using the $E_p = 1747.6 \pm 0.9$ keV resonance in the $^{13}\text{C}(p,\gamma)^{14}\text{N}$ reaction (60).

2.2 Targets and Target Chamber:

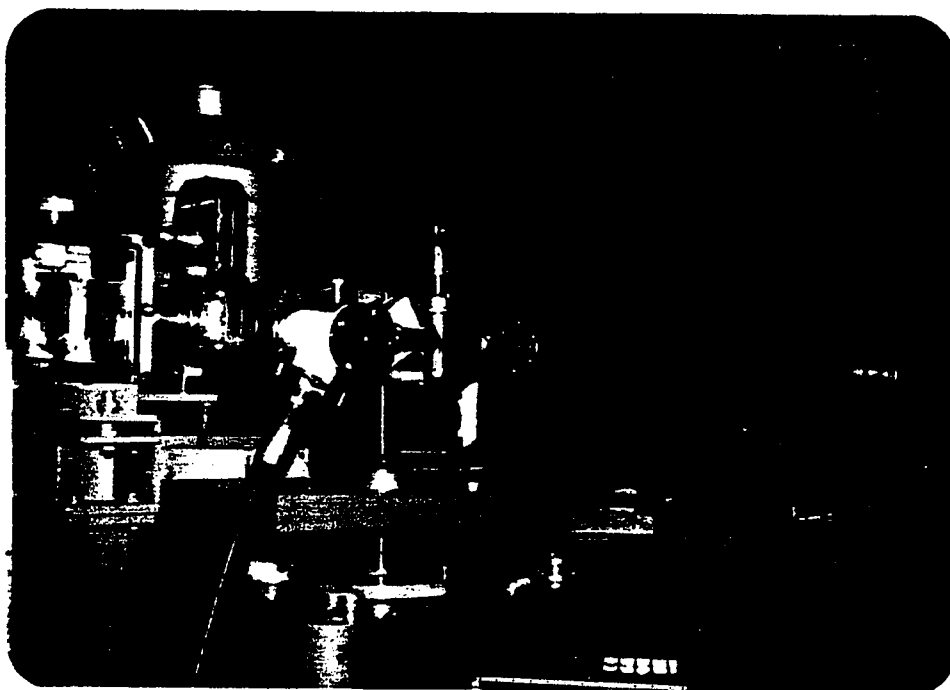
Two sets of ^{56}Fe (99,93% enrichment) targets were used in collecting the data. The first set was $26\mu\text{g}/\text{cm}^2$ on 0.13 mm thick tantalum backing and the second set was a $20\mu\text{g}/\text{cm}^2$ on a $20\mu\text{g}/\text{cm}^2$ carbon and gold foil.

The target chamber was a 5 cm in diameter aluminum cylinder which was fixed at the center of the angular distribution table (fig. 3(a)). To minimize the unwanted reactions due to the scattering of protons at the target chamber walls, tantalum sheets were used as a lining on the inner walls of the target chamber. The target chamber was electrically insulated and used as a Faraday cup for measuring the beam charge. During the experiment targets were cooled using methanol water solution passing through tubings around the target holder.

During the measurement of the excitation function



(a) Target Chamber and Detectors



(b) Modified Target Chamber with Beam Extension

and γ -ray spectra, an extension tube (1 m long) was added to the beam line beyond the position of the target chamber (fig. 3(b)). This addition helped in reducing the background of unwanted contaminants and in lowering the dead time to within 5%.

2.3 Detectors and Electronics:

Three cylindrically coaxial Ge(Li) detectors were used to collect the data. The first has an active volume of 95 cm^3 , an effective efficiency of 19.1% at 25 cm source to detector distance (relative to a 3x3 inch NaI(Tl) detector) and its energy resolution is 1.95 keV (FWHM) for the 1333 keV γ -ray from ^{60}Co source. The second detector has an active volume of 48 cm^3 , a relative efficiency of 8% and an energy resolution of 1.87 keV (FWHM) for the 1333 keV γ -ray from ^{60}Co source. The third detector has an active volume of 45 cm^3 and an energy resolution of 2.2 keV (FWHM) for the 1333 keV γ -ray from ^{60}Co radioactive source.

The first (95 cm^3) detector was used as a movable while the second (48 cm^3) was used as a monitor in collecting most of the data presented in this thesis. At a later stage of data collection and due to some problems with the

energy resolution of the 95 cm³ detector, the 48 cm³ detector (movable) and the 45 cm³ detector (monitor) were used in collecting some of the data.

Figure 4 shows the block diagram of the detectors and the electronics which were used in collecting the data. Pulses from the detectors were stored either in a 4K TN1700 multichannel analyzer or in an online PDP-15 computer. All data was recorded on magnetic tapes for subsequent analysis. The overall detection system was checked and calibrated using ⁶⁰Co and ²²Na radioactive sources.

2.4 Excitation Function and γ -Ray Spectra:

In all the measurements described in this section, the ⁵⁶Fe target was placed at 45° and the Ge(Li) detector (shielded) at 55° with respect to the proton beam direction.

The excitation function was measured over proton energy range $E_p = 3694\text{--}3855$ keV in steps of 1.6 keV using the 26 μ g/cm² target and the 95 cm³ Ge(Li) detector. At each proton energy a γ -spectrum was collected for a charge of 200 μ C, and four gates were selected to indicate the γ -yields. Table 1 shows the selected gates and their energy ranges. The reproducibility of the excitation function was

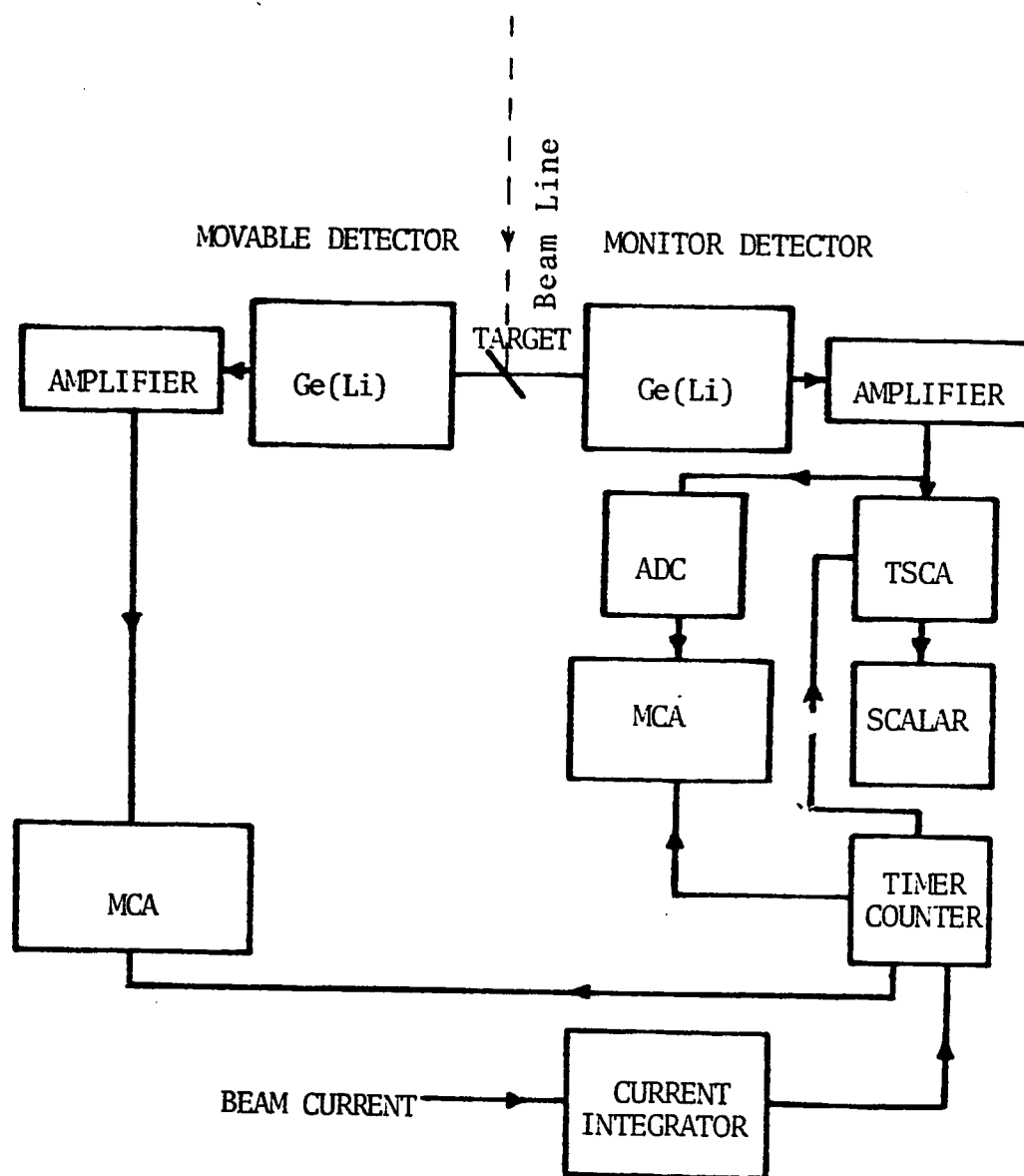


Figure 4 : Detectors and Electronics Block Diagram.

TABLE 1 : Selected Gates for γ -Ray Yield
in the Measurement of the
Excitation Function

Gate Number	γ -Ray Energy Range	Reaction (Transition)
1	8.6 - 10.0 MeV	$^{56}\text{Fe}(P,\gamma)^{57}\text{Co}$ ($g_{9/2} + \text{IAR} \rightarrow \text{G.S.}$) ($d_{5/2} + \text{IAR} \rightarrow \text{G.S.}$)
2	840 - 855 keV	$^{56}\text{F}(P,P^-\gamma)$ (846 keV(2+))
3	4.0 - 5.0 MeV	$^{56}\text{Fe}(P,\gamma)^{57}\text{Co}$ ($R \rightarrow T_{\angle}$)
4	7.0 - 10.0 MeV	$^{56}\text{Fe}(P,\gamma)^{57}\text{Co}$ ($R \rightarrow \text{G.S.}$ and $R \rightarrow \text{low energy states}$)

checked several times using the $20\mu\text{g}/\text{cm}^2$ target and the 48 cm^3 Ge(Li) detector.

Gamma-ray spectra were detected using the $26\mu\text{g}/\text{cm}^2$ ^{56}Fe target and the 95 cm^3 Ge(Li) detector at the $E_p=3720$, 3727 , 3774 and 3793 keV resonances. Off-resonance spectra were also measured at $E_p = 3712$ and 3786 keV to allow for background subtraction, proper analysis of the spectra and establishing the decay schemes. The γ -spectra at $E_p=3774$ 3793 and 3786 keV were also measured using the $20\mu\text{g}/\text{cm}^2$ ^{56}Fe target and the 48 cm^3 Ge(Li) detector.

Gamma-ray spectra were calibrated using ^{60}Co and ^{22}Na radioactive sources. The presence of the $6129.41\pm 0.18\text{ keV}$ γ -ray from the $^{19}\text{F}(\text{P},\alpha\gamma)^{16}\text{O}$ reaction as a contaminant (61) served as a calibration point for the higher energy portion of the spectra.

Peaks on the γ -spectra were identified and their centroids were determined. Sums were obtained for each of the photo-peak, single and double escapes of each γ -ray after proper subtraction of background. The sums of γ -yields were then corrected by subtracting the off-resonance contribution and correcting the net intensity of each γ -ray for detector efficiency. The decay scheme for each resonant state was then established and their branching ratios were

determined. The error in the decay scheme branching ratios ranges from 1 to about 2%. All of the γ -ray spectra analysis was accomplished using a FORTRAN program (see appendix C) on the UPM 3033 IBM Computer.

2.5 *Gamma-Ray Angular Distributions:*

Gamma-ray spectra were measured at four angles between 0° and 90° relative to the proton beam direction at each of the $E_p = 3720, 3774$ and 3793 keV resonances. The movable detector (shielded and collimated) was placed at 7 cm distance from the target while the monitor detector (shielded) was at 90° with respect to the beam direction and situated 4 cm from the target.

The gamma-ray angular distribution at the $E_p=3720$ keV resonance was measured using the $26\mu\text{g}/\text{cm}^2$ ^{56}Fe target, the 95 cm^3 Ge(Li) detector (movable) and the 48 cm^3 Ge(Li) detector (monitor). For the other two resonances ^{56}Fe target of $26\mu\text{g}/\text{cm}^2$ was used, the 48 cm^3 Ge(Li) detector (movable) and the 45 cm^3 Ge(Li) detector (monitor).

The anisotropy of the angular distribution table was measured using the 844 keV (2^+) γ -ray arising from the $^{27}\text{Al}(p,p'\gamma)$ reaction which has an isotropic angular distribution. The anisotropy correction resulted from such

measurement was found to be within 1% which was used in correcting the angular distribution data.

The sum of the areas under the full energy, single and double escape peaks after proper background subtraction was taken to be proportional to the γ -ray intensity. These areas were normalized with respect to the monitor and corrected for the anisotropy of the angular distribution table.

The measured intensities obtained at the four angles were fitted using a least squares procedure to the theoretical distribution described by the factored formalism of Harris et al. (62). The angular distribution data presented here were analyzed with the aid of a computer program which is a simple version of the program discussed by Hyder et al. (63). The general correlation function in this program is given in terms of population parameters defining the relative populations of the magnetic substates of the state being populated in the reaction. For unpolarized protons bombarding a spin-zero target, as is the case for $^{56}\text{Fe}(\text{p},\gamma)^{57}\text{Co}$ reaction studied here, only one parameter (the multipole mixing ratio δ) enters the least squares fit of the experimental data to the theoretical expressions (appendix A).

The angular distribution results were analyzed to determine those spins and mixing ratios which minimize the function $Q^2 = (1/N) \sum_i \frac{1}{\Delta W_i} \{W(\theta_i) - W^*(\theta_i)\}^2$ where N is the number of degrees of freedom, ΔW_i is the statistical error at each angle, $W(\theta_i)$ is the experimental counting rate measured at the i th angle θ_i and $W^*(\theta_i)$ is the theoretical counting rate at θ_i . The quantity $W^*(\theta_i)$ is a function of the assumed spins and multipole mixing ratios.

For each possible spin assignment, the value of Q^2 was calculated for values of the multipole mixing ratio δ between $-\infty$ and $+\infty$. In actual practice the substitution $x = \arctan \delta$ is employed and values of Q^2 are calculated in 2° steps in x . In the case where there is a statistically significant agreement between the experimental data and the theory the minimum value of Q^2 is near unity. Hence acceptable solutions for the spin of the level and δ are those for which Q^2 can be made approximately equal to unity. The 0.1% limit at $Q^2 = Q_0^2$ for example indicates there is a statistical probability of 0.001 that the correct solution will have a measured value of Q^2 which is greater than or equal to Q_0^2 . The estimates of errors associated with the mixing ratio δ were obtained at $Q^2 = Q_0^2$ corresponding to one standard deviation from Q_{\min}^2 .

CHAPTER 3

RESULTS AND DISCUSSION

3.1 Excitation Function:

Figure 5 shows the excitation function of the ^{56}Fe (P, γ) and ^{56}Fe (P,P γ) reactions at the four different gates (mentioned earlier) in the $E_p=3694\text{--}3855$ keV range. From the excitation function there are four strong resonances at $E_p=3720$, 3727, 3774 and 3793 keV. Other resonances in the 4-5 MeV gate are due to the 5270 keV contaminant γ -ray arising from the ^{18}O (P, $\alpha\gamma$) reaction (64). The doublet at $E_p=3720$ and 3727 keV has been observed in earlier (P, γ) experiments by Fodor et al. (56) at $E_p=3727$ and 3735 keV, and by Rangacharyulu et al. (57) at $E_p=3721$ and 3728 keV.

3.2 Gamma-Ray Spectra and Angular Distribution:

From the excitation function it is clear that the four resonances at $E_p=3720$, 3727, 3774 and 3793 keV show transitions to the ground state ($J^\pi=7/2^-$) as well as other states around the 4-5 MeV excitation in ^{57}Co . These four resonances are discussed in the next two sections.

3.2.1 Resonances at $E_p=3720$ and 3727 keV:

Figure 6 shows the high energy portion of the γ -ray spectra at $E_p=3720$ and 3727 keV resonances as well as an off resonance spectrum at $E_p=3712$ keV.

The decay scheme of both resonances including the branching ratios is shown in fig. 7. As it is evident from the decay scheme both resonances populate high spin states in ^{57}Co . The state at 4586 keV could be identified with the one observed by Rosner and Holbrow (48) at 4600 ± 20 keV from $^{56}\text{Fe}(^3\text{He},d)^{57}\text{Co}$ reaction.

Table(2) shows a comparison between the γ -decay and branching ratios for both resonant states as a result of the present work and those reported earlier by Fodor et al.(56) and Rangacharyulu et al. (57).

Based on the mode of decay of the $E_p=3720$ keV resonance, transitions to the ground, 4586 and 2611 keV states have been used in the analysis of the angular distribution data. The least squares fits to angular distributions assuming different spin values for the three transitions studied at the $E_p=3720$ keV resonance are shown in fig. 8.

The Q^2 analysis of the $R\rightarrow G.S.$ angular distribution data (fig.9) indicates that the spin value for this

resonant state at $E_x=9682$ keV is either $5/2$ (with $\delta = -0.176 \pm 0.011$) or $9/2$ (with $\delta=0.035 \pm 0.011$).

Comparison of the mixing ratios δ , determined from fitting the theoretical expression to the angular distribution data with the single-particle transition strength (Weisskopf estimate), allows an upper limit to be placed on the multipolarity of the γ -radiation. It may be possible from such comparisons to reject some mixing ratios or even spin assignments. It is also sometimes possible to make a parity assignment on this basis. Table 3 summarizes the results of such comparisons for the three transitions studied at the $E_p=3720$ keV resonance.

Considering the resonance to G.S. transition (see table 3), a $J^\pi=5/2^\pm$ assignment can be ruled out when compared with the single particle transition strengths (Weisskopf estimate). A $J^\pi=9/2^-$ for this resonance is also very unlikely using a similar argument as above (see table 3). However, a $J^\pi=9/2^+$ is assigned for this resonant state at $E_x=9682$ keV.

Fodor et al. (56) have studied the same resonance and from their angular distribution measurement for the $R \rightarrow$ G.S. transition, a $J^\pi=9/2^+$ has been assigned, which is in

agreement with the present work. Rangacharyulu et al. (57) who investigated the same energy range ruled out a possible $J^\pi=9/2^+$ on the basis of the γ -ray mode of decay at this proton energy; consequently they did not attempt any angular distribution measurement.

On the basis of $J^\pi=9/2^+$ for the $E_p=3720$ keV resonance, the $R\rightarrow 4586$ keV Q^2 -fits (fig. 10) indicate that the only acceptable spin value for the level at 4586 keV is $9/2$ with $\delta = 0.035\pm 0.02$. Based on the Weisskopf estimate, a positive parity is very likely (see table 3) and consequently a $J^\pi=9/2^+$ is assigned to the 4586 keV level. This assignment is supported by the $^{56}\text{Fe}(^3\text{He},d)^{57}\text{Co}$ data of Rosner and Holbrow (48) who identified an $\ell_p=4$ at $E_x=4600\pm 20$ keV in ^{57}Co . On similar basis Fodor et al. (56) inferred a $J^\pi=9/2^+$ for a level at 4585 keV.

Using $J^\pi=9/2^+$ for this resonant state, the $R\rightarrow 2611$ keV transition Q^2 -fits indicate that a $J=7/2$ with $\delta=0.035\pm 0.013$ is the only acceptable spin value for the state at $E_x=2611$ keV in ^{57}Co . Figure 11 shows the results of the Q^2 -fits for the $R\rightarrow 2611$ keV transition. From the Weisskopf estimate (see table 3) a negative parity is more likely, and a $J^\pi=7/2^-$ is assigned for the 2611 keV state. Previous (P,γ) experiments on ^{56}Fe targets failed to assign a unique spin value for this

state (44).

Concerning the $E_p=3727$ keV resonance, a $J^\pi=9/2^+$ is most likely based on the mode of decay of the resonant state at $E_x=9689$ keV. Angular distribution measurement at $E_p=3727$ keV resonance by Fodor et al. (56) and by Ranga-charyulu et al. (57) resulted in a $J^\pi=9/2^+$ which agrees with the J^π value inferred from the decay scheme results discussed earlier. (see fig. 7).

3.2.2 Resonances at $E_p=3774$ and 3793 keV:

Figure 12 shows the high energy portions of the γ -ray spectra at $E_p=3774$ and 3793 keV resonances as well as an off-resonance spectrum at $E_p=3786$ keV. The decay of both resonances including the branching ratios is shown in fig. 13.

For the resonance at $E_p=3774$, angular distribution analysis was performed for transitions from the resonant state to G.S., 1378, 1757 and 4675 keV levels in ^{57}Co . Figure 14 shows the least squares fits of these angular distributions assuming different spin values.

For the $R \rightarrow \text{G.S.}$ transition, Q^2 analysis (fig. 15)

indicates that the spin of this resonant state could be either $3/2$ or $5/2$. However, comparison with the Weisskopf estimate (table 4) shows that the spin and parity of this resonant state at $E_X=9734$ keV is $\frac{5}{2}^+$.

The Q^2 results of the $9734 \rightarrow 1378$ keV transition is shown in fig. 16. From the fitting, spin values of $3/2$ and $5/2$ are considered acceptable. However, when these values were compared with the Weisskopf estimate (table 4) a $J^\pi = \frac{5}{2}^+$ for this resonance was assigned.

Figure 17 shows the Q^2 analysis for the $9743 \rightarrow 1757$ keV transition at the $E_p=3774$ keV resonance. Comparison of the experimental mixing ratio values with the Weisskopf estimate confirms the $J^\pi = \frac{5}{2}^+$ for the resonant state at $E_X=9734$ keV (see table 4).

On the basis of $J^\pi = 5/2^+$ for the resonant state at $E_X=9734$ keV, the $R \rightarrow 4675$ keV Q^2 -fit (fig. 18) indicated that a $J=3/2$ and $5/2$ were acceptable for the 4675 keV state. However, the $J=3/2$ value was ruled out by comparison of the δ values with the Weisskopf estimate (table 4) and a $J^\pi = 5/2^+$ was taken as most probable for the 4675 keV state.

For the resonance at $E_p=3793$ keV ($E_X=9753$ keV), angular distribution analysis was performed for transitions

from the resonant state to the G.S., 1897 and 4675 keV levels in ^{57}Co . Figure 19 shows the least squares fits of these angular distributions assuming different spin values.

The Q^2 -fit (fig. 20) for the $R \rightarrow \text{G.S.}$ transition allows two possible spin values for the resonant state, $5/2$ and $3/2$. However, after comparison with the Weisskopf estimate (table 5) a $J^\pi = 3/2^+$ or $5/2^+$ could be assigned to the $E_x = 9753$ keV state.

Figure 21 shows the Q^2 -fit for the $R \rightarrow 1897$ keV transition. Comparison of the mixing ratios from the Q^2 analysis with the Weisskopf estimate (table 5) indicates that a $J^\pi = 5/2^+$ assignment for this resonant state is very likely.

The $R \rightarrow 4675$ keV transition was analyzed using the assigned $J = 5/2^+$ for the resonant state at $E_x = 9753$ keV. Comparing the results of the Q^2 -fit (fig. 22) with the Weisskopf estimate (table 5), confirms the $J^\pi = 5/2^+$ for the 4675 keV state assigned earlier.

3.3 Identification of Isobaric Analogue Resonances:

Identifying analogue states which are produced by

(P, γ) reactions, or which happen to be excited bound states of the nucleus can be particularly difficult when the analogue strength is split up and mixed into some other nuclear substructure. The identification may then depend on recognizing various features of the nuclear states, such as coulomb displacement energy (ΔE_C), common spins and parities for closely spaced levels in the parent nucleus.

Based on the coulomb displacement energy $\Delta E_C = 8876 \pm 6$ keV (54) for the ^{57}Co - ^{57}Fe pair the doublet at $E_p = 3720$ and 3727 keV is identified as the split analogue of the $E^* = 2455$ keV, $J^\pi = 9/2^+$ parent state in ^{57}Fe . The state $E = 4586$ keV in ^{57}Co is identified as the antianalogue $J^\pi = 9/2^+$ state. The other two resonances at $E_p = 3774$ and 3793 keV are identified as the fragmented analogue resonances of the $E^* = 2506$ keV, $J^\pi = 5/2^+$ state. Table 6 summarizes a comparison between the resonances found in the present work with those expected for analogues of ^{57}Fe states.

3.4 *Summary and Conclusions:*

As a result of the work presented in this thesis, spins and parities of the $E_p = 3720$, 3774 , 3793 keV resonances in ^{57}Co have been determined from angular distribution measurements. A $J^\pi = 9/2^+$ has been assigned for the resonance at $E_p = 3720$ keV, while a $J^\pi = 5/2^+$ has been assigned for the

two resonances at $E_p=3774$ and 3793 keV. From the γ -spectrum and mode of decay a $J^\pi=9/2^+$ has been assigned for the $E_p=3727$ keV resonance. Moreover, the spin and parity of the levels at $E_x=2611$, 4586 and 4675 keV in ^{57}Co have been determined as $J^\pi=7/2^-$, $9/2^+$ and $5/2^+$ respectively. Figure 23 summarizes the results presented in this thesis.

The spins and parities of these resonances along with their energy spacings as obtained from the $^{56}\text{Fe}(p,\gamma)^{57}\text{Co}$ excitation function and the coulomb displacement energy $\Delta E_c=8876\pm 6$ keV have been used in identifying these resonances as analogue states to the 2455 keV ($J^\pi=9/2^+$) and the 2506 keV ($J^\pi=5/2^+$) states in ^{57}Fe . The resonances at $E_p=3720$ and 3727 keV ($J^\pi=9/2^+$) have been identified as the fragmented analogue of the 2455 keV ($J^\pi=9/2^+$) state in ^{57}Fe . The $E_p=3774$ and 3793 keV resonances have been identified as the fragmented analogue of the 2506 keV ($J^\pi=5/2^+$) state in ^{57}Fe .

The levels at 4586 keV ($J^\pi=9/2^+$) and 4675 keV ($J^\pi=5/2^+$) in ^{57}Co have been identified as antianalogue ($T^<$) states.

Concerning the doublet at $E_p=3720$ and 3727 keV, the present results indicate that the $g_{9/2}$ analogue resonance in ^{57}Co is split into two fragments contrary to earlier

results by Rangacharyulu et al. (57) who rejected the $E_p = 3720$ keV resonance from being a $g_{9/2}$ analogue candidate. However, the present results are in agreement with those reported by Fodor et al. (56).

In conclusion, the analogue to antianalogue M1 strength tend to be strongly reduced for both $g_{9/2}$ and $d_{5/2}$ analogue resonances in ^{57}Co compared to the 2s-1d shell nuclei. Such departure from the single-particle picture is a direct consequence of the core polarization effects on the antianalogue state. Admixture of core polarized components into the antianalogue state can be especially effective in reducing analogue to antianalogue M1 transition strength if both the odd particle and the perturbing core have $J = \ell + 1/2$. The present work indicates that many of the properties of other lighter 1f-2p shell nuclei such as ^{49}Sc and ^{51}V are reproduced in the ^{57}Co nucleus. Similar investigation on ^{59}Co nucleus indicated that the $g_{9/2}$ IAR are severely fragmented to the extent that they escaped observation (66). Briefly the analogue antianalogue M1 strength reaches a maximum in the middle of the 1f-2p shell nuclei and tends to decrease on either side. Qualitatively such decrease in M1 strength near the closure of the $1f_{7/2}$ proton shell could be understood as a result of the increased core polarization with the increase of the mass number in this region of nuclei.

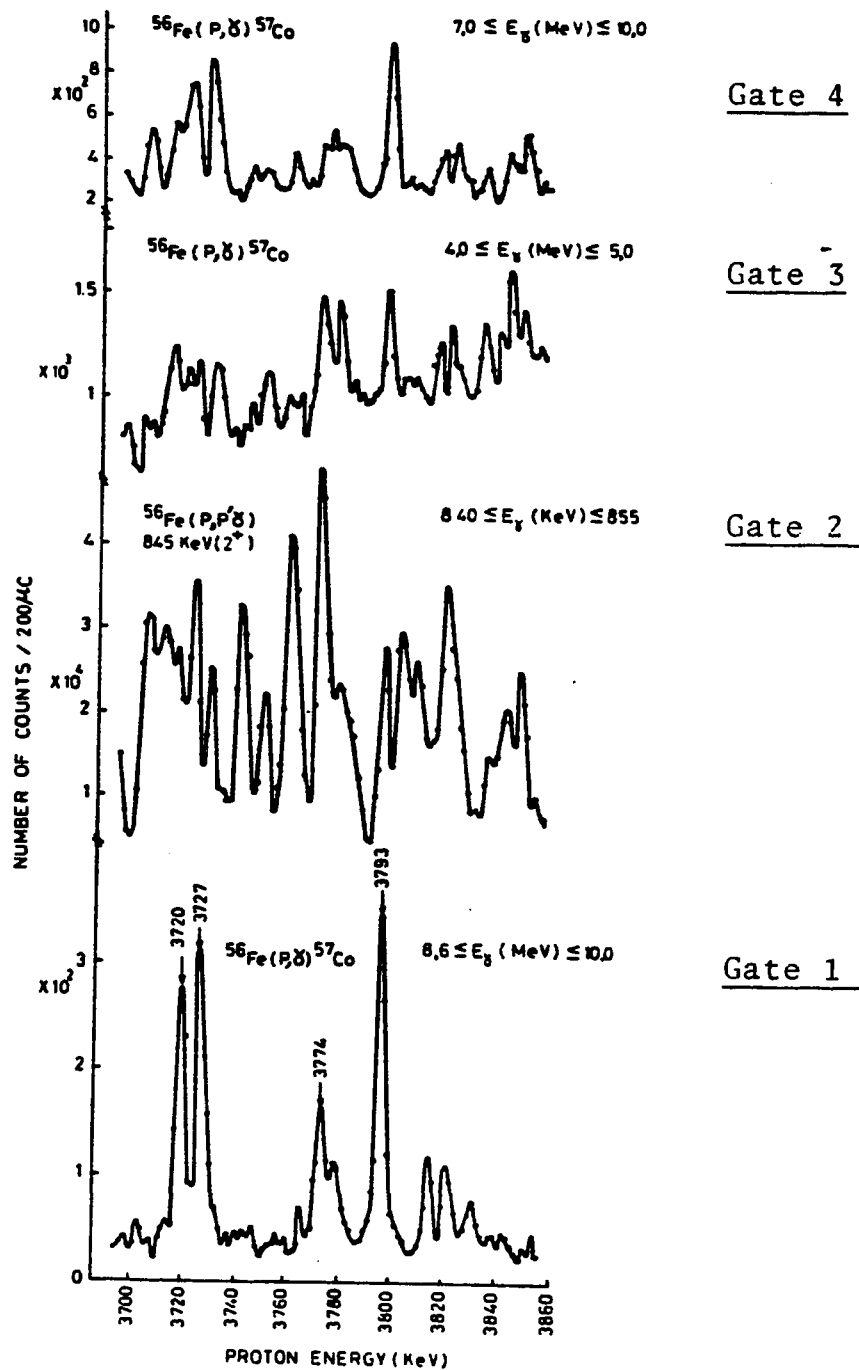


Figure 5 : Excitation function for $E_p = 3694\text{--}3855$ keV. Four γ -ray energy gates are shown above. The target used in this measurement was $20 \mu\text{g}/\text{cm}^2$.

Figure 6 : High energy portion of the γ -ray spectra at the $E_p=3720$ and 3727 keV resonances and an off-resonance at $E_p=3712$ keV. All three spectra were measured with a 95 cm³ Ge(Li) detector.

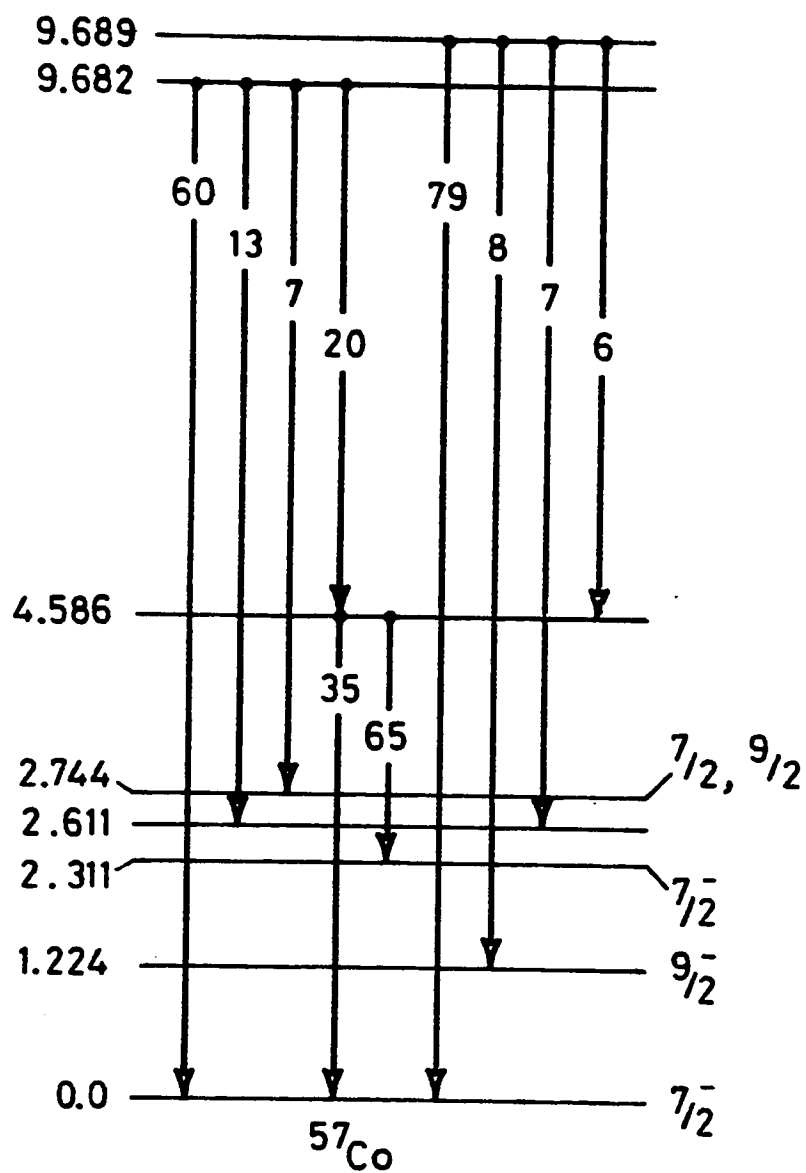


Figure 7 : The decay scheme of the resonances at $E_p = 3720$ and 3727 keV.

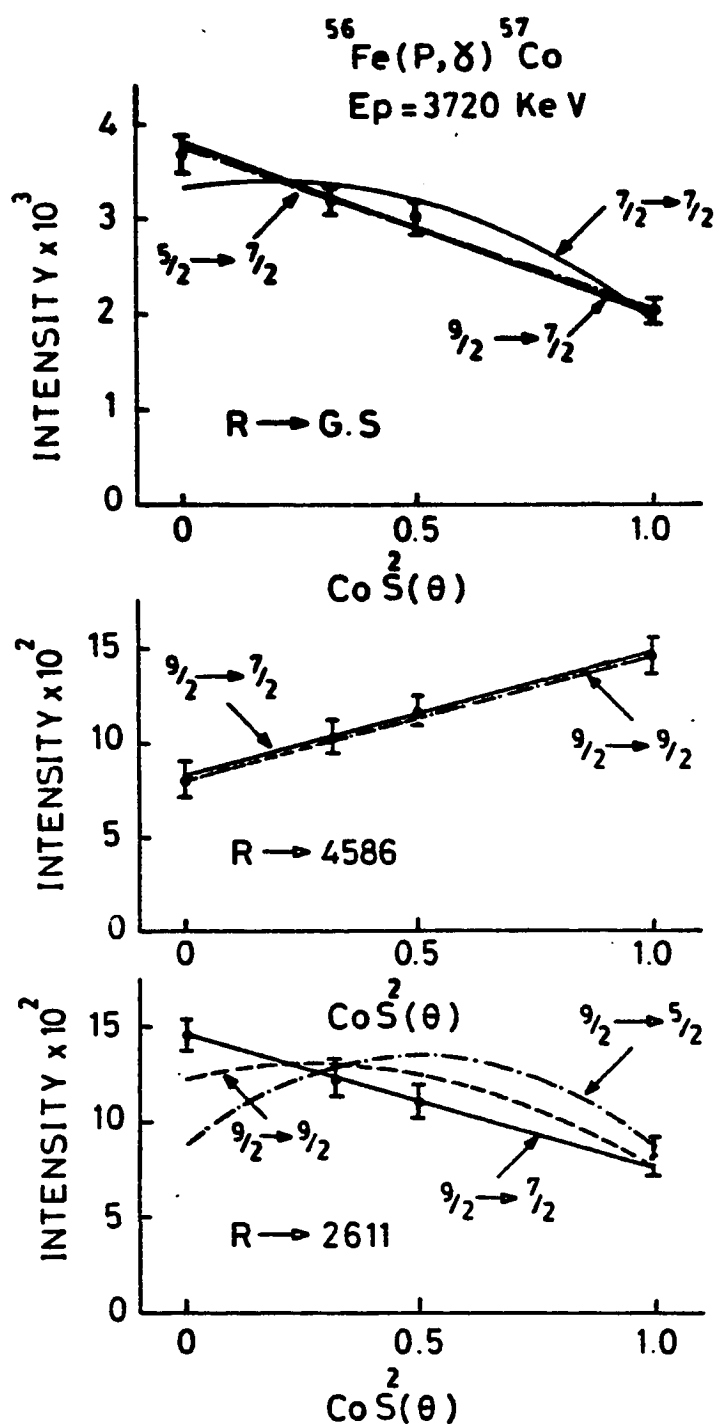


Figure 8 : Experimental angular distribution data and their Least Squares fits for Different spin Sequences.

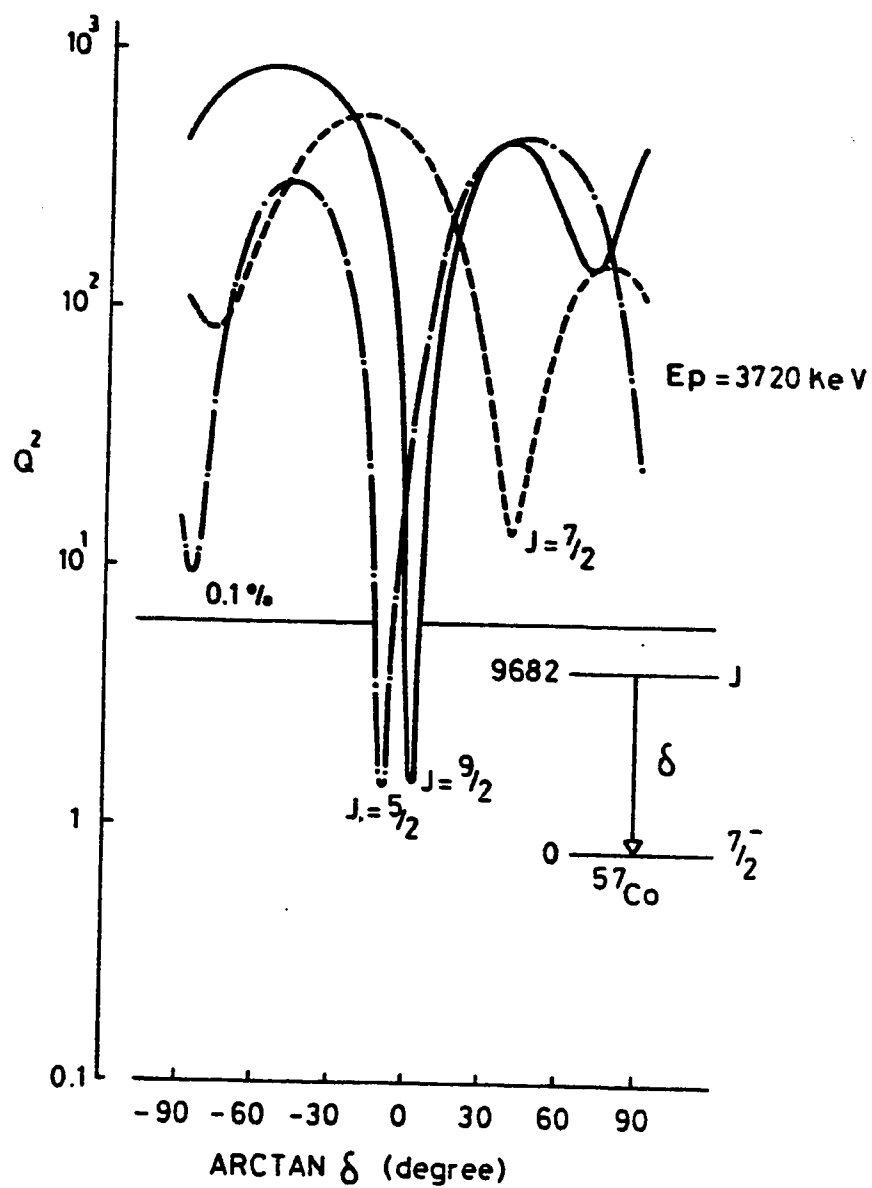


Figure 9 : Values of Q^2 versus $\text{arctan } \delta$ from fitting experimental angular distribution of R to G.S. transition to theory for different spin values.

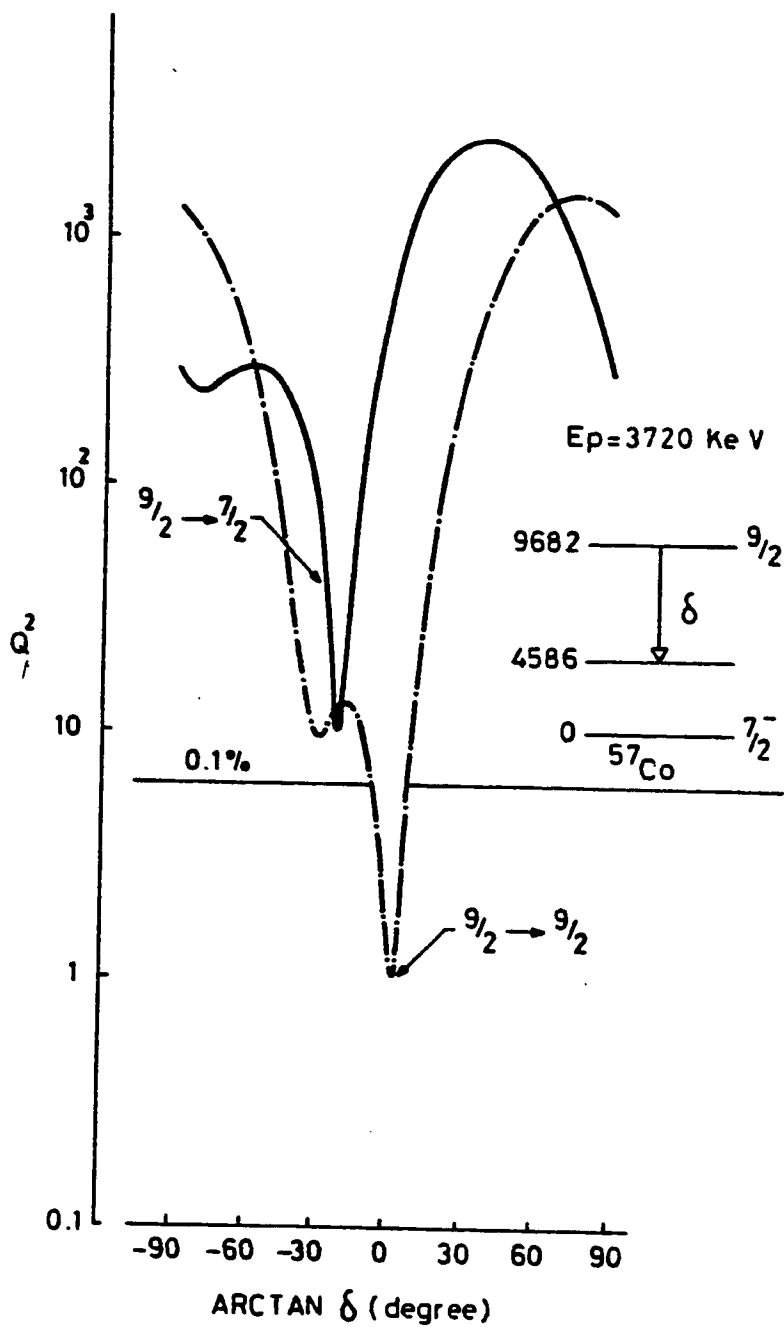


Figure 10 : Values of Q^2 versus $\text{arctan } \delta$ from fitting Experimental angular distribution of R to 4586 keV transition to theory for different spin values.

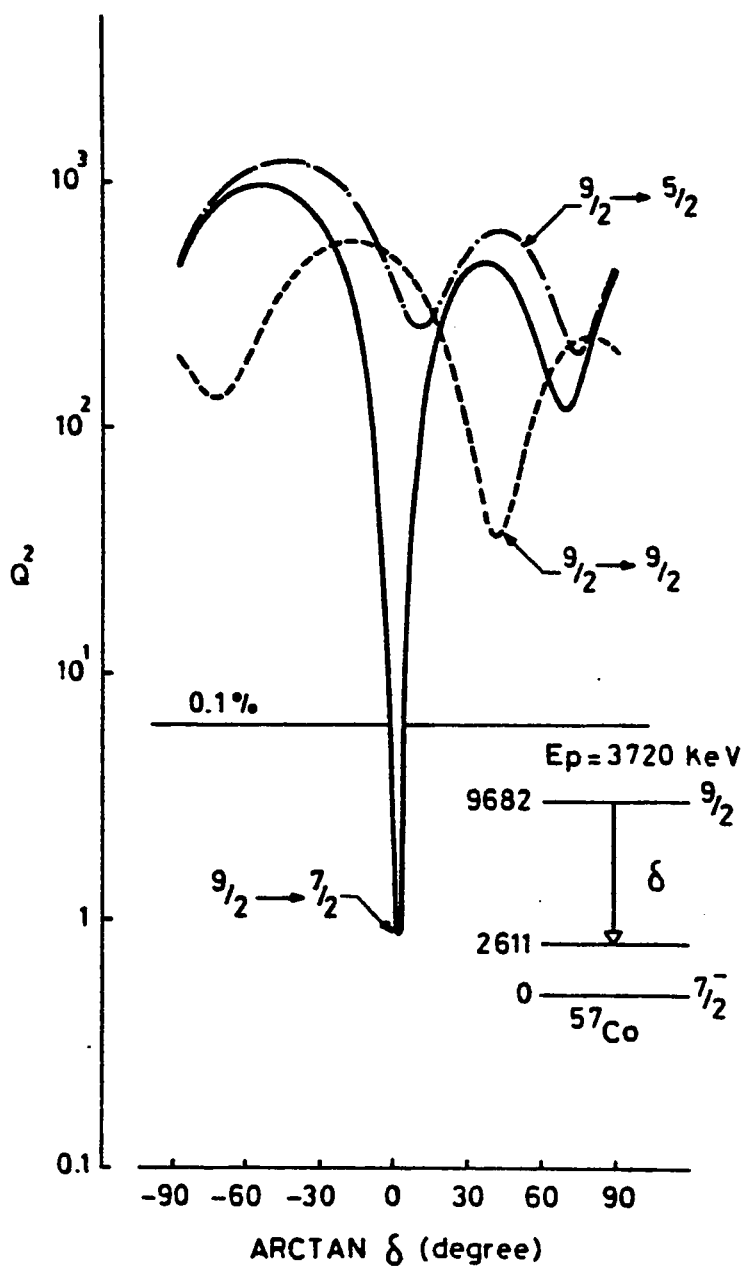


Figure 11 : Values of Q^2 versus $\text{arctan } \delta$ from fitting experimental angular distribution of R to 2611 keV transition to theory for different spin values.

Figure 12 : High energy portion of the γ -Ray spectra at the $E_p=3774$ and 3793 keV resonances and an off-resonance at $E_p=3786$ keV. All three spectra were measured using a 48 cm³ Ge(Li) Detector.

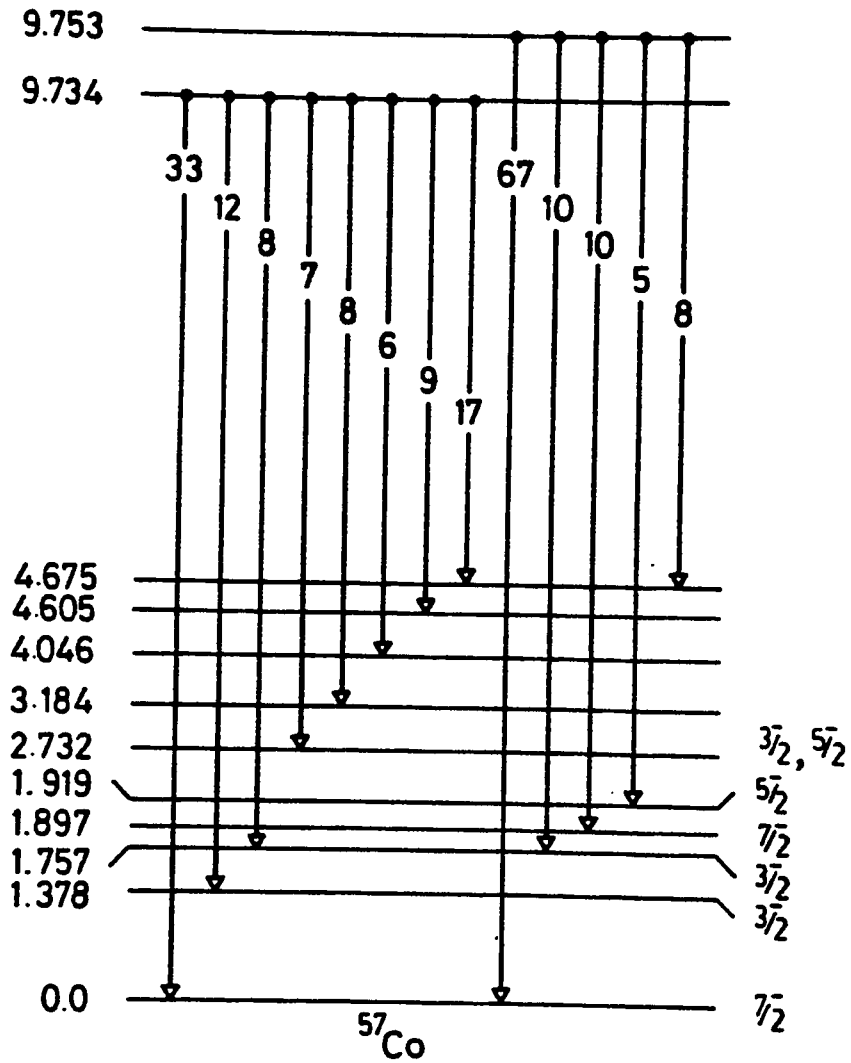


Figure 13 : The decay scheme of the resonances at $E_p=3774$ and 3793 keV.

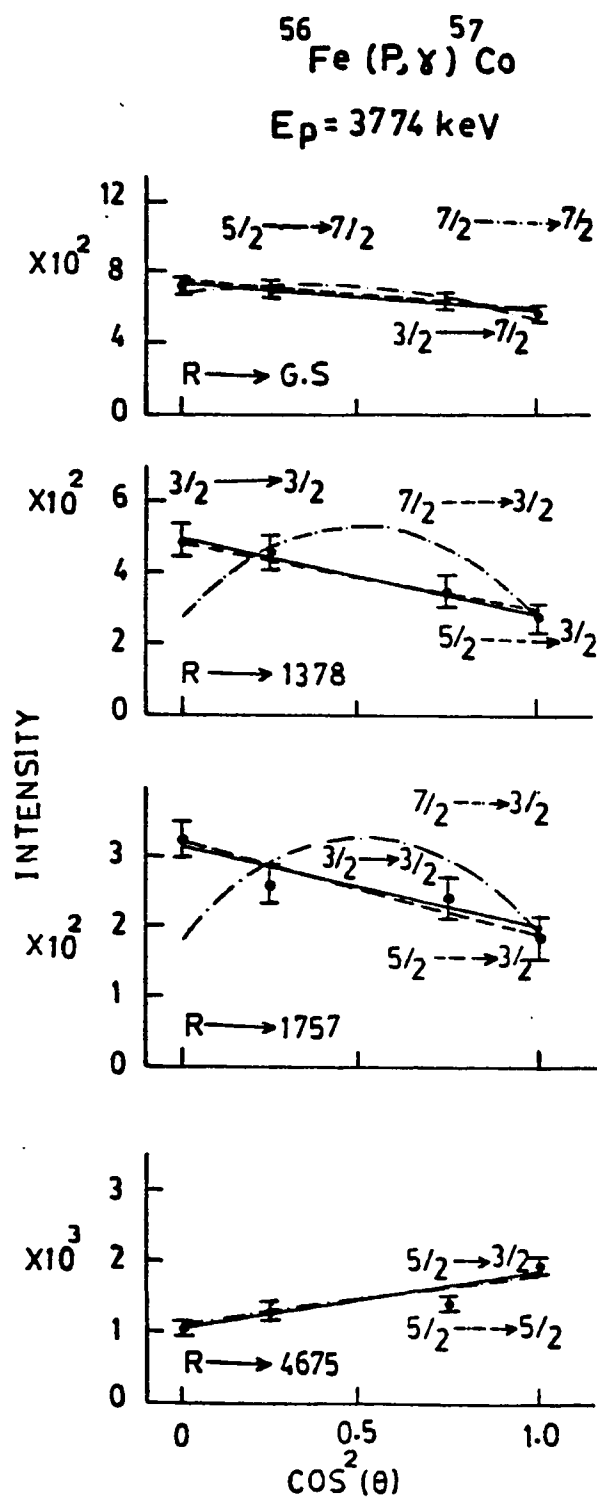


Figure 14 : Experimental angular distribution data and their Least Squares Fits to different spin sequences.

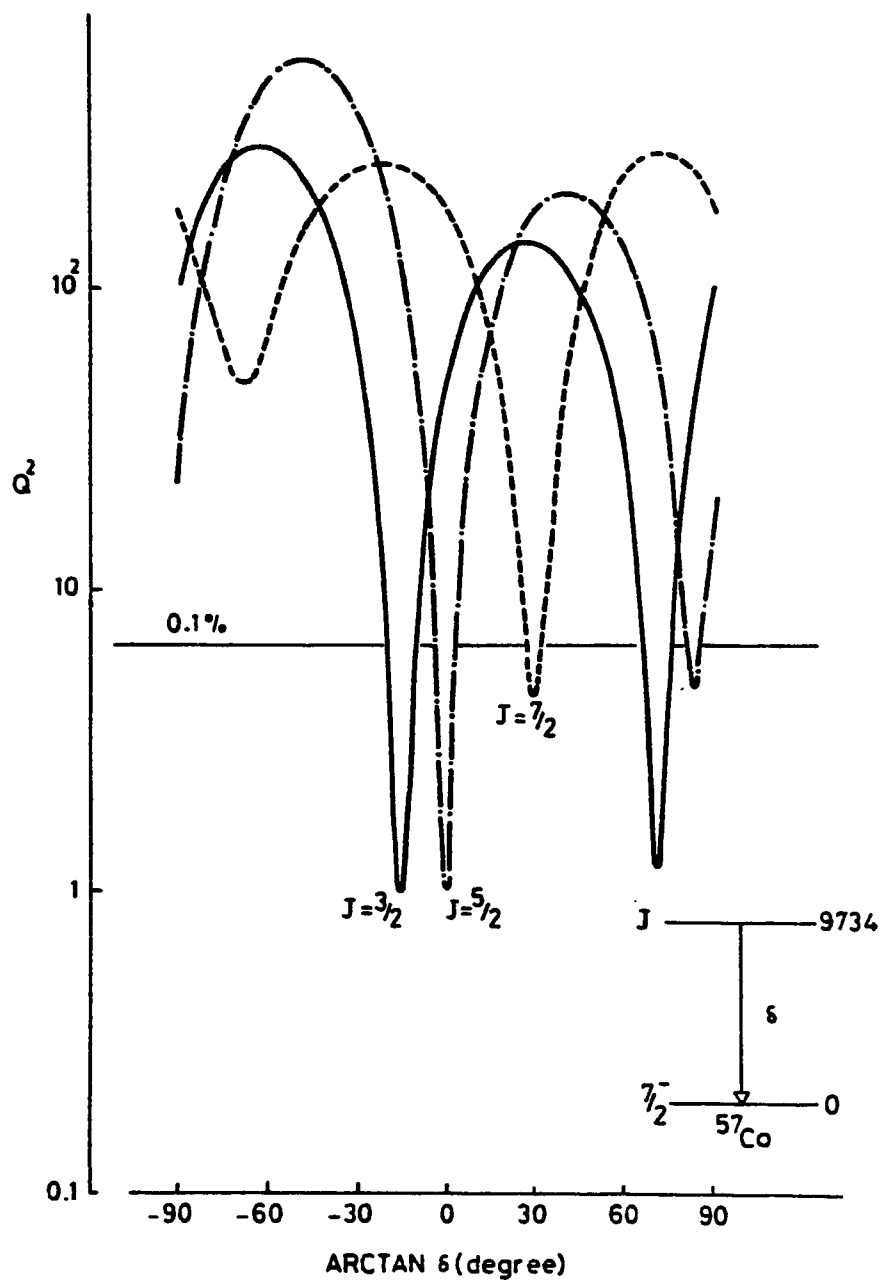


Figure 15 : Values of Q^2 versus $\text{arctan } \delta$ from fitting experimental angular distribution of R to G.S. transition to theory for different spin values.

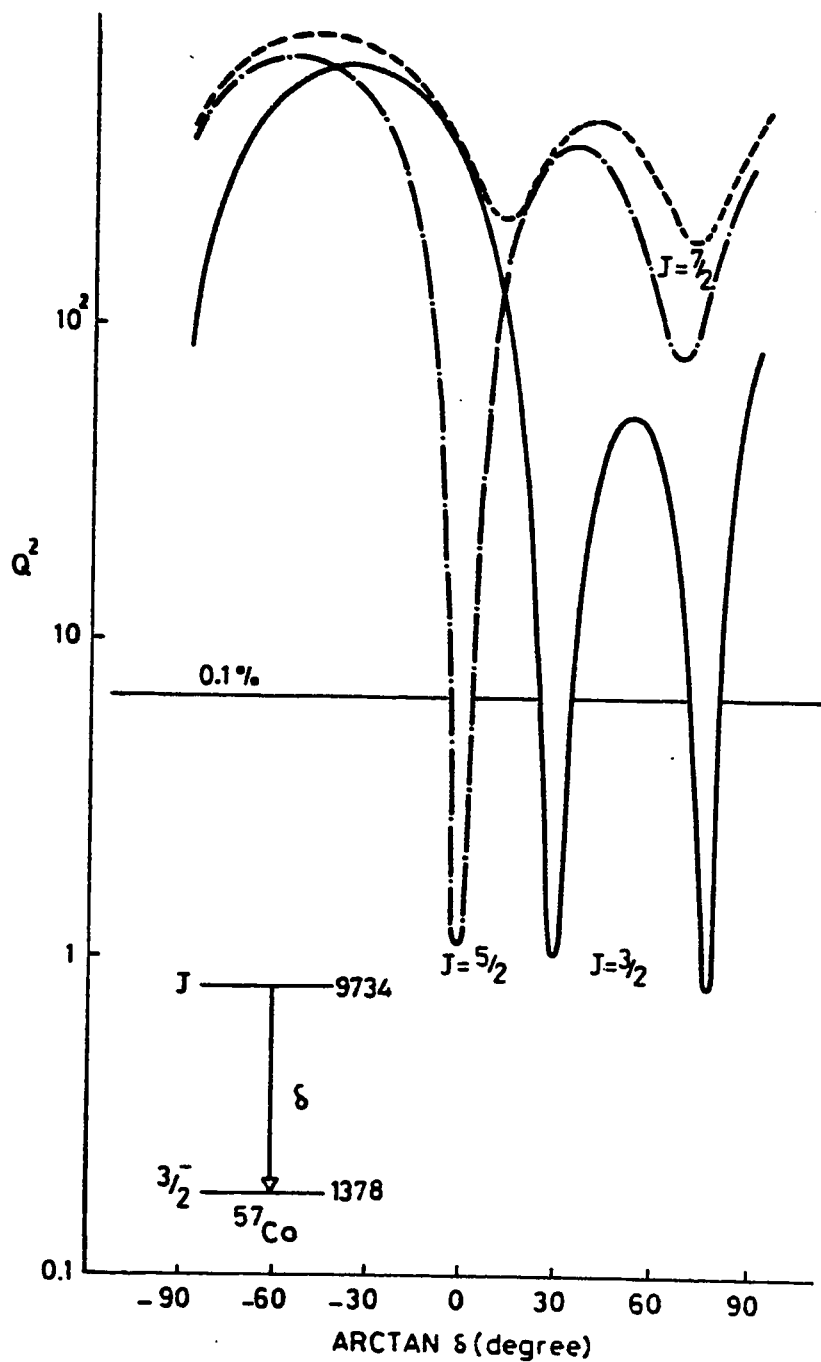


Figure 16: Values of Q^2 versus $\text{arctan } \delta$ from fitting experimental angular distribution of R to 1378 keV transition to theory for different spin values.

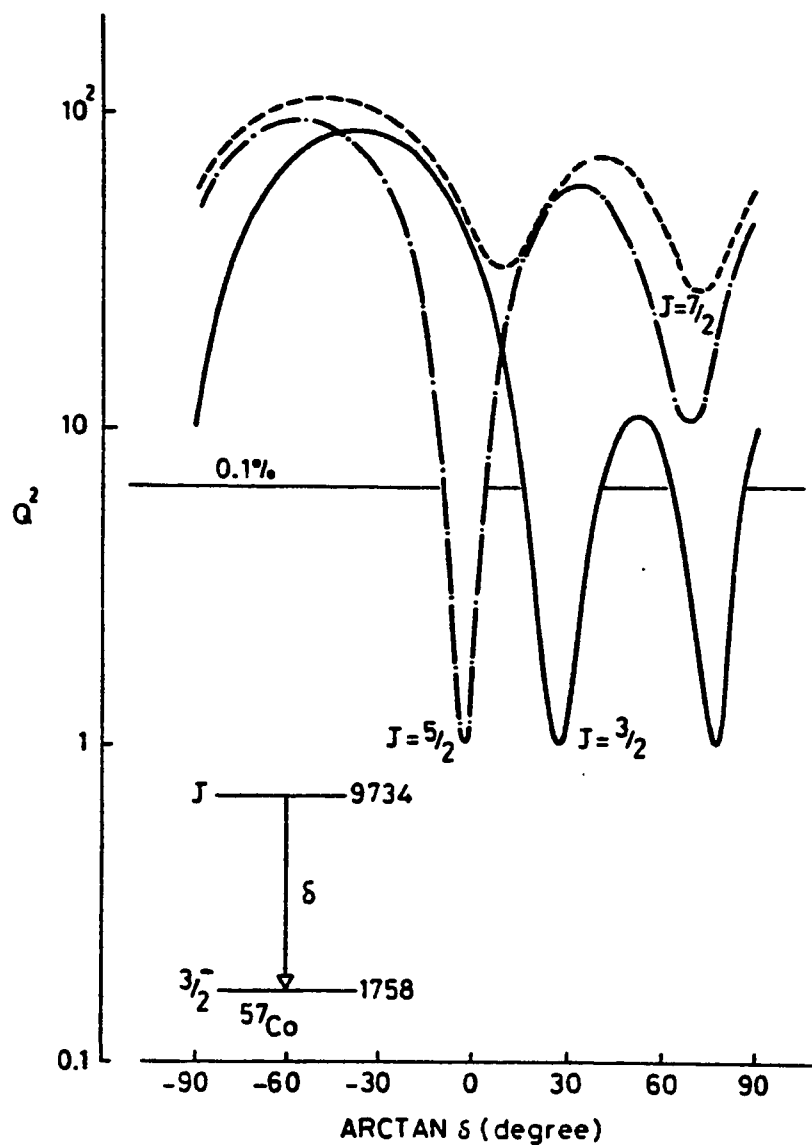


Figure 17 : Values of Q^2 Versus $\text{arctan } \delta$ from fitting experimental angular distribution of R to 1758 keV transition to theory for different spin values.

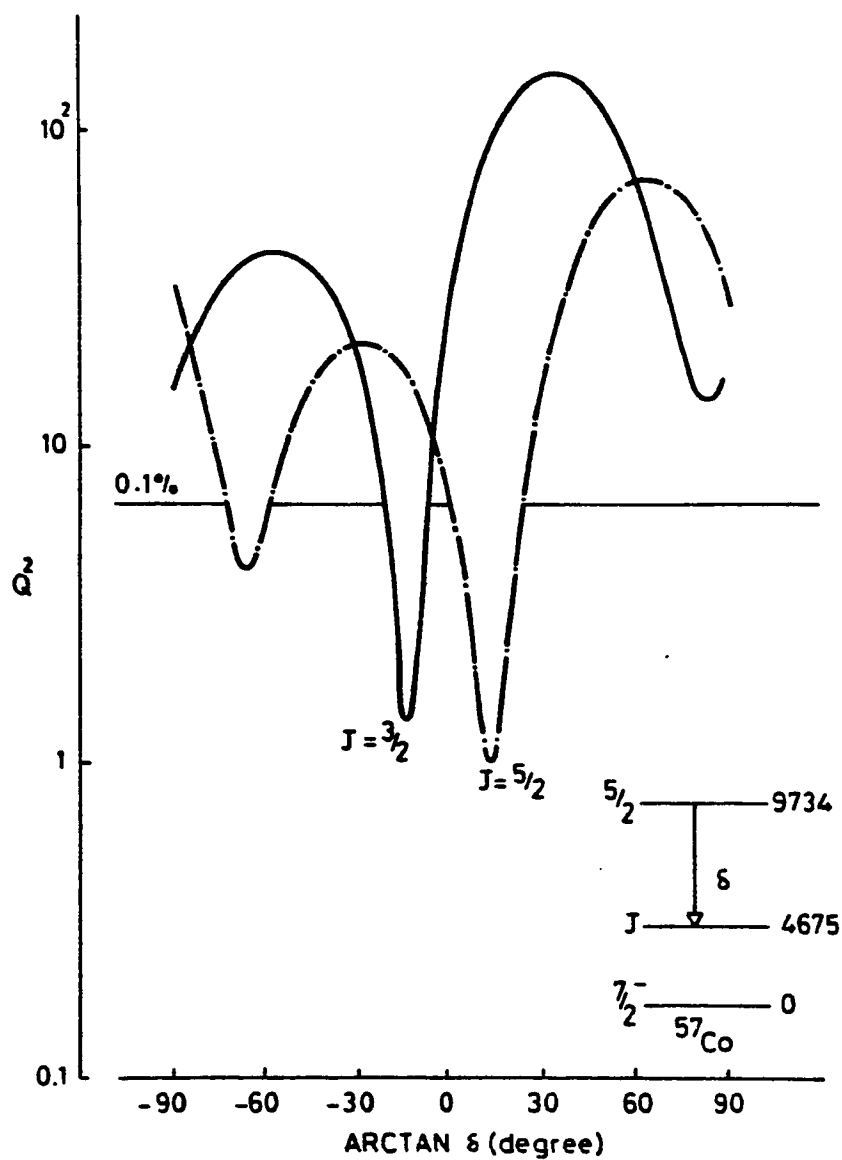


Figure 18 : Values of Q^2 Versus $\arctan \delta$ from fitting experimental angular distribution of R to 4675 transition to theory for different spin values.

$^{56}\text{Fe}(\text{P},\gamma)^{57}\text{Co}$

49

$E_p = 3793 \text{ keV}$

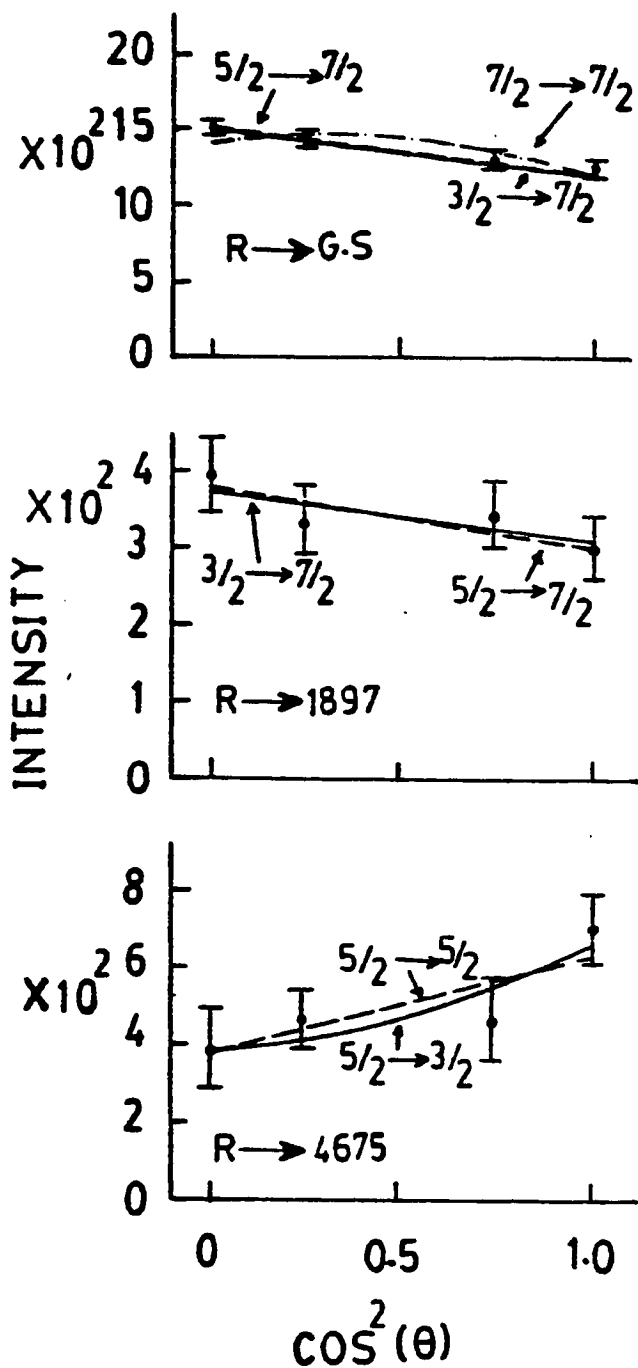


Figure 19 : Experimental angular distribution data and their Least Squares fits for different spin sequences.

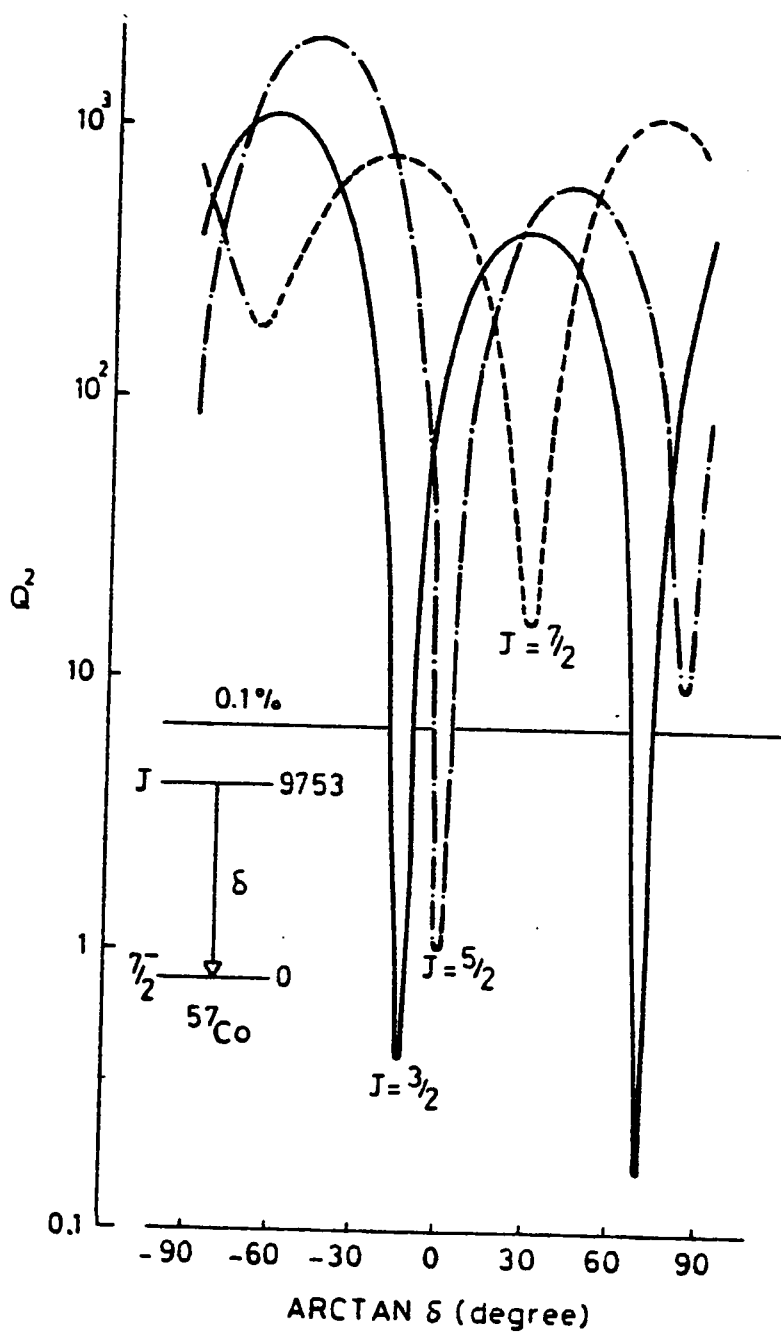


Figure 20 : Values of Q^2 versus $\arctan \delta$ from fitting experimental angular distribution of R to G.S. transition to theory for different spin values.

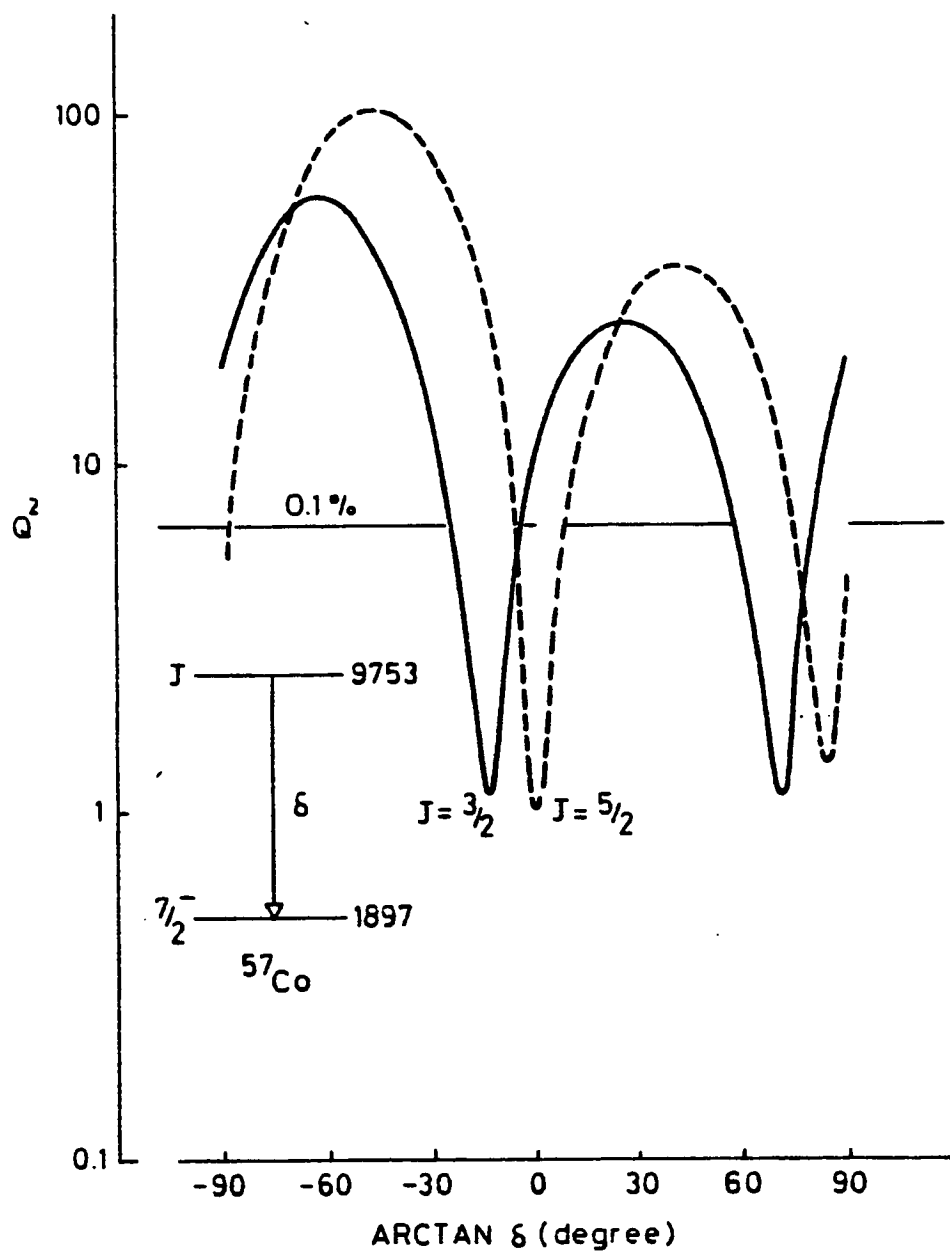


Figure 21 : Values of Q^2 versus $\arctan \delta$ from fitting experimental angular distribution of R to 1897 keV transition to theory for different spin values.

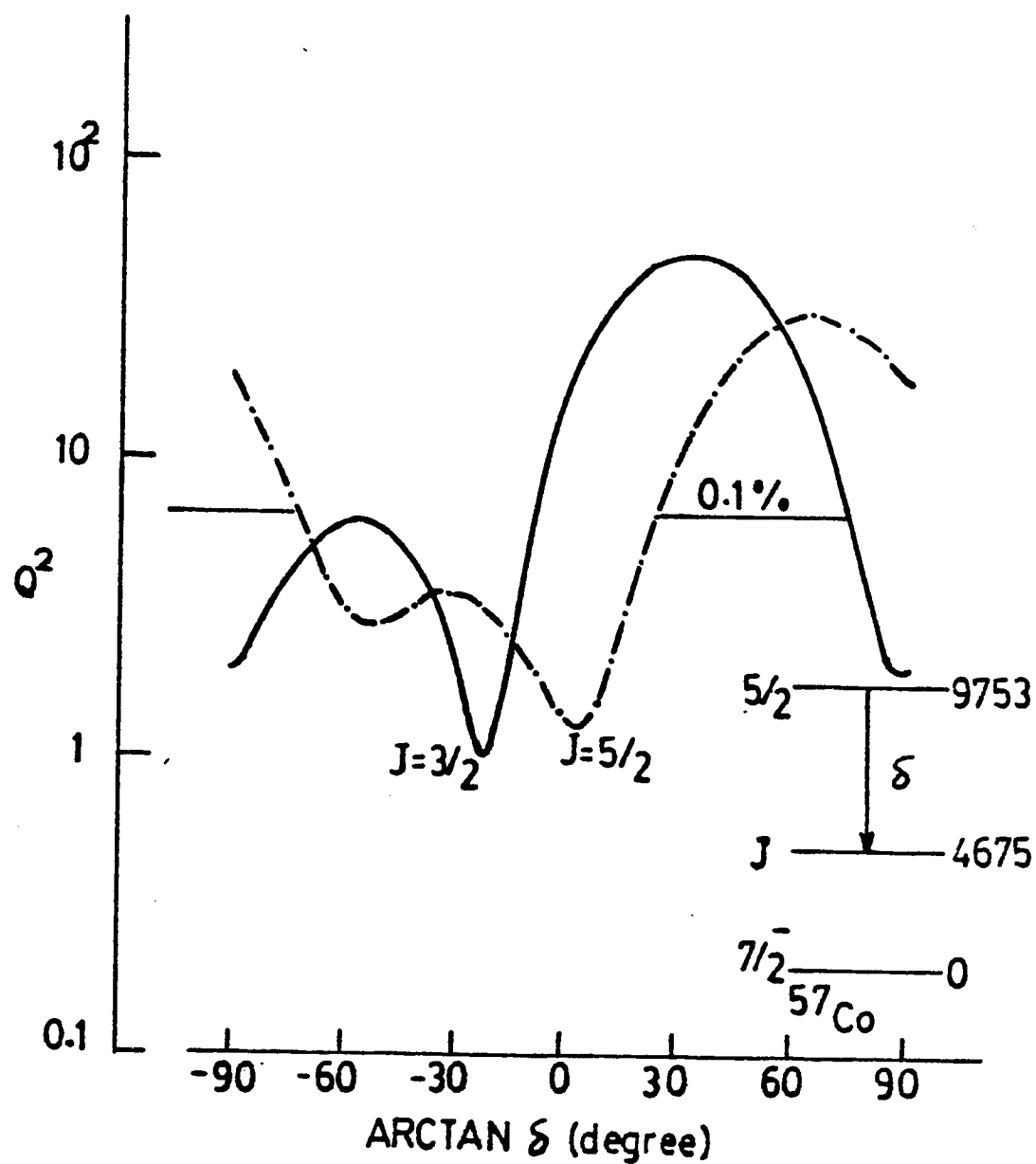


Figure 22 : Values of Q^2 Versus $\arctan \delta$ from fitting experimental angular distribution of R to 4675 keV transition to theory for different spin values.

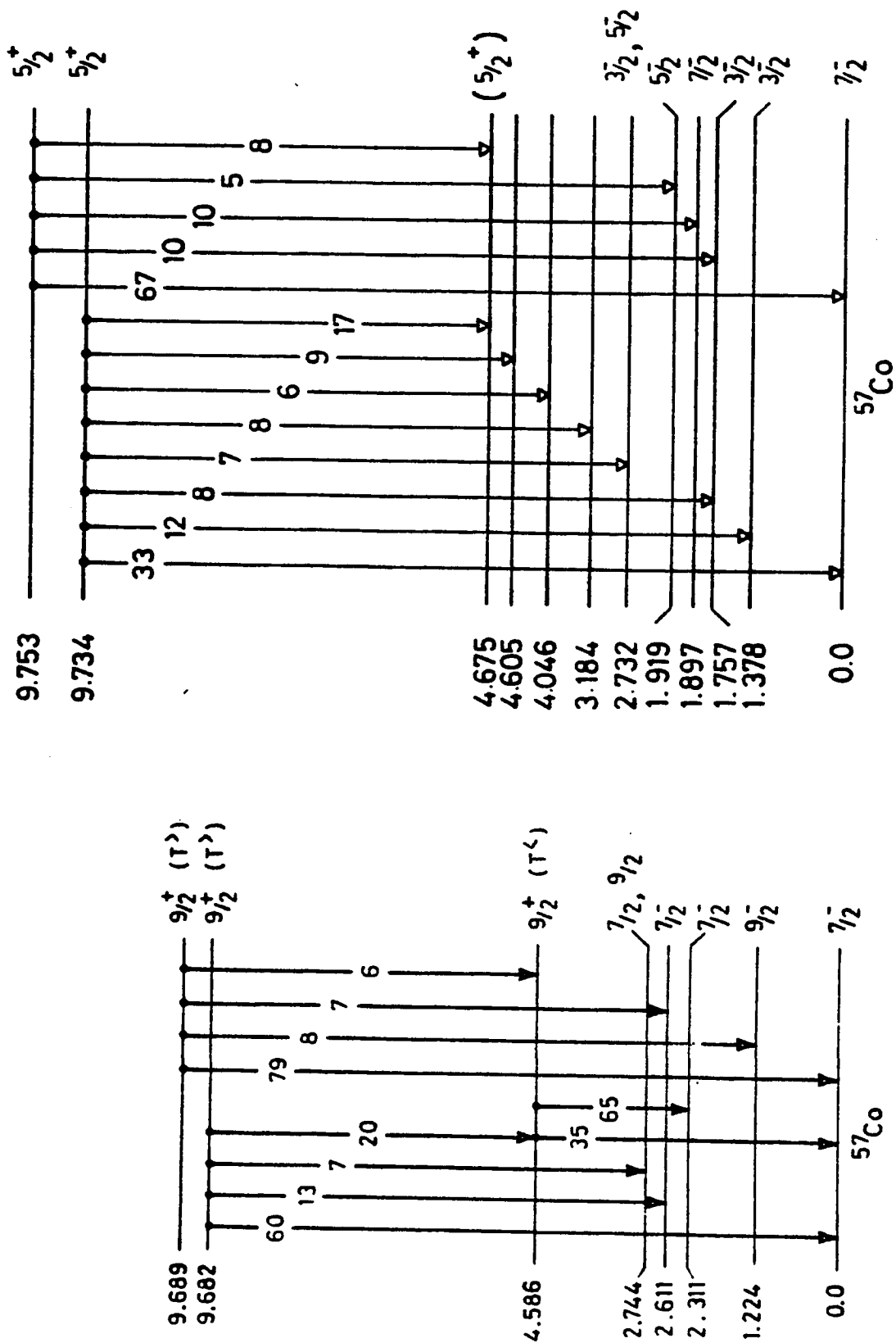


Figure 23 : Decay schemes and spin assignments for $E_x=9682$, 9689, 9734 and 9753 keV resonant states in ^{57}Co .

TABLE 2 : Comparison Between Branching Ratios of the $g_{9/2}$ IAR as a Result of the Present Study With Those Reported Earlier.

Transition	Resonance at $E_p=3720$ keV			Resonance at $E_p=3727$ keV		
	Fodor et al. (ref 56)	Rangacharyulu et al.(ref 57)	Present work	Fodor et al. (ref 56)	Rangacharyulu et al.(ref 57)	Present work
R + G.S.	70%	(Strong) No value quoted	60%	74%	70%	79%
R + 1223					15%	8%
R + 1757		(Strong) No value quoted				
R + 2311					15%	
R + 2611	6%		13%	6%		7%
R + 2723	4%			5%		
R + 2744	4%		7%	4%		
R + 4586	16%		20%	11%		6%

TABLE 3 : Experimental Mixing Ratios δ Compared with Weisskopf Values for the Transitions Studied at the $E_p=3720$ keV Resonance.

Transition $E_i \rightarrow E_f$ (keV)	$J_i \rightarrow J_f^\pi$	Character	Weisskopf Estimate for $ \delta $	Experimental Mixing Ratios δ	Assigned J_f^π
9682 \rightarrow G.S.	$5/2^+ \rightarrow 7/2^-$	E1 (M2)	0.0045	-0.176 ± 0.011	$J_i^\pi = 9/2^+$
	$5/2^- \rightarrow 7/2^-$	M1 (E2)	0.2190	-0.176 ± 0.011	
	$9/2^+ \rightarrow 7/2^-$	E1 (M2)	0.0045	0.035 ± 0.011	
	$9/2^- \rightarrow 7/2^-$	M1 (E2)	0.2190	0.035 ± 0.011	
9682 \rightarrow 4586	$9/2^+ \rightarrow 9/2^-$	E1 (M2)	0.0024	0.035 ± 0.020	$J_f^\pi = 9/2^+$
	$9/2^+ \rightarrow 9/2^+$	M1 (E2)	0.11	0.035 ± 0.020	
9682 \rightarrow 2611	$9/2^+ \rightarrow 7/2^-$	E1 (M2)	0.0033	0.035 ± 0.013	$J_f^\pi = 7/2^-$
	$9/2^+ \rightarrow 7/2^+$	M1 (E2)	0.1600	0.035 ± 0.013	

TABLE 4 : Experimental Mixing Ratios δ Compared with Weisskopf Values
for the transitions studied at the $E_p=3774$ keV Resonance.

Transition $E_i \rightarrow E_f$ (keV)	$J_i \rightarrow J_f^\pi$	Character	Weisskopf Estimate for $ \delta $	Experimental Mixing Ratios δ	Assigned J_i^π
9734 \rightarrow G.S.	$5/2^- \rightarrow 7/2^-$	M1(E2)	0.2202	0.0 ± 0.01	$J_i^\pi = 5/2^+$
	$5/2^+ \rightarrow 7/2^-$	E1(M2)	0.0046	0.0 ± 0.01	
	$3/2^- \rightarrow 7/2^-$	E2(M3)	0.0036	-0.287 ± 0.006	
	$3/2^+ \rightarrow 7/2^-$	M2(E3)	0.1785	-0.287 ± 0.006	
9734 \rightarrow 1378	$5/2^- \rightarrow 3/2$	M1(E2)	0.1890	-0.035 ± 0.035	$J_i^\pi = 5/2^+$
	$5/2^+ \rightarrow 3/2^-$	E1(M2)	0.0039	-0.035 ± 0.035	
	$3/2^- \rightarrow 3/2^-$	M1(E2)	0.1890	0.53 ± 0.03	
	$3/2^+ \rightarrow 3/2^-$	E1(M2)	0.0039	0.53 ± 0.03	

Continued...

TABLE 4 (continued)

Transition $E_i \rightarrow E_f$ (keV)	$J_i \rightarrow J_f^\pi$	Character	Weisskopf Estimate for $ \delta $	Experimental Mixing Ratios δ	Assigned J^π
9734 \rightarrow 1757	$5/2^- \rightarrow 3/2^-$	M1 (E2)	0.1805	-0.035 ± 0.035	$J_i^\pi = 5/2^+$
	$5/2^+ \rightarrow 3/2^-$	E1 (M2)	0.0037	-0.035 ± 0.035	
	$3/2^- \rightarrow 3/2^-$	M1 (E2)	0.1805	0.53 ± 0.07	
	$3/2^+ \rightarrow 3/2^-$	E1 (M2)	0.0037	0.53 ± 0.035 0.07	
9734 \rightarrow 4675	$5/2^+ \rightarrow 5/2^-$	E1 (M2)	0.0024	$0.070 \pm .07$ $.11$	$J_f^\pi = 5/2^+$
	$5/2^+ \rightarrow 5/2^+$	M1 (E2)	0.1145	$0.070 \pm .07$ $.11$	
	$5/2^+ \rightarrow 3/2^-$	E1 (M2)	0.0024	$-0.404 \pm .05$	
	$5/2^+ \rightarrow 3/2^+$	M1 (E2)	0.1145	$-0.404 \pm .05$	

TABLE 5 : Experimental Mixing Ratios δ Compared with Weisskopf Values
for the Transitions Studied at the $E_p = 3793$ keV Resonance.

Transition $E_i \rightarrow E_f$ (keV)	$J_i \rightarrow J_f^\pi$	Character	Weisskopf Estimate for $ \delta $	Experimental Mixing Ratios δ	Assigned J_f^π
9753 \rightarrow G.S.	$5/2^- \rightarrow 7/2^-$	M1(E2)	0.2207	$0.0 \pm .03$	$J_i^\pi = 5/2^+$ $= 3/2^+$
	$5/2^+ \rightarrow 7/2^-$	E1(M2)	0.0046	$0.0 \pm .03$	
	$3/2^+ \rightarrow 7/2^-$	M1(E2)	0.2207	$-0.249 \pm .017$	
	$3/2^+ \rightarrow 7/2^+$	E1(M2)	0.0046	-0.249 ± 0.017	
9753 \rightarrow 1897	$5/2^- \rightarrow 7/2^-$	M1(E2)	0.1777	$0.0 \pm .035$	$J_i^\pi = 5/2^+$
	$5/2^+ \rightarrow 7/2^-$	E1(M2)	0.0037	$0.0 \pm .035$	
	$3/2^- \rightarrow 7/2^-$	E2(M3)	0.0029	$-0.249 \pm .035$	
	$3/2^+ \rightarrow 7/2^-$	M2(E3)	0.1441	$-0.249 \pm .035$	
9753 \rightarrow 4675	$5/2^+ \rightarrow 3/2^-$	E1(M2)	0.0024	-0.404 ± 0.05	$J_f^\pi = 5/2^+$
	$5/2^+ \rightarrow 3/2^+$	M1(E2)	0.1149	-0.404 ± 0.05	
	$5/2^+ \rightarrow 5/2^-$	E1(M2)	0.0024	$-0.0699 \pm .09$ $.12$	
	$5/2^+ \rightarrow 5/2^+$	M1(E2)	0.1149	$0.0699 \pm .09$ $.12$	

TABLE 6 : Comparison of the Resonances Studied in the Present Work with those expected for Analogues of States of ^{57}Fe .

Parent States in ^{57}Fe		Expected Analogue States in ^{57}Co			Observed Analogue States in ^{57}Co		
E^* (keV)	J^π	E_x (keV)	E_p (keV)	J^π	E_x (keV)	E_p (keV)	J^π
2455	$9/2^+$	9712	3707	$9/2^+$	9682 9689	3720 3727	$9/2^+$ $9/2^+$
2506	$5/2^+$	9763	3758	$5/2^+$	9734 9753	3774 3793	$5/2^+$ $5/2^+$

APPENDIX "A"

60

ANGULAR CORRELATION FORMALISM

Many books and review articles have been published discussing the formalism of angular correlation (67-71).

In the factored formalism, the notation used follows closely the notation of Smith (68,69). The angular distribution data presented in the present work on $^{56}\text{Fe}(p,\gamma)^{57}\text{Co}$ were analyzed using this factored formalism. For a two step gamma-ray cascade (Figure 24), the angular correlation function specifying the relative intensity $W(\theta_1, \theta_2, \phi)$ can be written as:

$$W(\theta_1, \theta_2, \phi) = \sum_{KMN} A_{KM}^N Q_K Q_M X_{KM}^N(\theta_1, \theta_2, \phi) \quad (1)$$

where θ_1 and θ_2 are the angles between the propagation vectors of the incoming beam and of the primary and secondary radiation and ϕ is the relative azimuthal angle between them. The Q_K and Q_M are finite geometry detector correction factors. The functions $X_{KM}^N(\theta_1, \theta_2, \phi)$ are the angular functions and defined as:

$$X_{KM}^N = [(2M+1)(2K+1)(K-N)!(M-N)! / (K+N)!(M+N)!]^{1/2} P_K^N(\cos\theta_1) P_M^N(\cos\theta_2) \cos N\phi \quad (2)$$

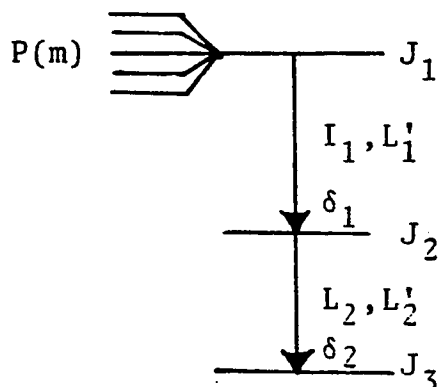


Figure 24 : Schematic energy level diagram to illustrate the quantum numbers used for a double gamma-ray cascade from an aligned nuclear state.

Under the conditions of defined parities and sharp spin of all levels, and of unpolarized bombarding particles and target, K and M can take on even integral values, K takes all even integral values up to the order of the highest multipolarity occurring in the primary transition of the cascade, i.e. $|L_1 - L_1'| \leq K \leq L_1 + L_1'$. M is limited by either the multipolarity of the second member of the cascade or the spin J_2 of the intermediate level, whichever is smaller, i.e. $M \leq \min. (L_2' + L_2', J_2 + J_2')$. N may take any positive value from zero to the smallest of K and M . $P_K^N(\cos\theta_1)$ and $P_M^N(\cos\theta_2)$ are the associated Legendre polynomials, where the associated Legendre polynomials, can each be expressed as a sum of the ordinary Legendre polynomials as:

$$P_V^N(\cos\theta) = \sum_k P_{VK}^N P_k(\cos\theta)$$

where $V=K$ or M and k is even and does not exceed K or M .

The expansion coefficient A_{KM}^N , characterizes a certain spin sequence, e.g. $J_1 \rightarrow J_2 \rightarrow J_3$. In the population parameter representation this coefficient is given by:

$$A_{KM}^N = \sum_{m \geq 0} P(m) \frac{\sum_{L_1 L_1' L_2 L_2'} \delta_1^{p_1} \delta_2^{p_2} C_{KM}^N}{(3)} \quad (3)$$

where

$$C_{KM}^N = \beta (-)^f (2J_1+1)(2J_2+1)(2L_1+1)^{\frac{1}{2}} (2L_1'+1)^{\frac{1}{2}} (2L_2+1)^{\frac{1}{2}} \\ (2L_2'+1)^{\frac{1}{2}} \langle L_1 \ 1 \ L_1' -1 \mid KO \rangle \langle L_2 \ 1 \ L_2' -1 \mid MO \rangle W(J_2 L_2 J_2 L_2'; J_3 \\ M) \sum_k (-1)^{J_1 - m} \langle J_1 m J_1 -m \mid KO \rangle \langle K -N \ M \ N \mid KO \rangle F(L_1')$$

where

$$F(S) = \begin{vmatrix} J_2 & L_1 & J_1 \\ J_2 & S & J_1 \\ M & K & k \end{vmatrix} \quad (4)$$

where $(-)^f$ is a phase factor where $f = J_3 - J_3 - J_2 + L'_1 - L_2 + L'_2 + M + N$ and β is a multiplicity term where $\beta = (2 - \delta_{N,0})(2 - \delta_{L_1, L'_1})(2 - \delta_{L_2, L'_2})$. In the A_{KM}^N expansion given by equation (3), P_1 and P_2 take on the values 0, 1 or 2 for pure L, mixed L, L' or pure L' radiation. The quantities δ_1 and δ_2 are the ratios of reduced matrix elements for L'-pole to L-pole radiation, i.e. $\delta_1 = \langle J_2 | L' | J_1 \rangle / \langle J_2 | L | J_1 \rangle$. $P_{(m)}$ is the population parameter of the substates +m plus that of substate -m. The δ in the β multiplicity term is the Kronecker delta. The C_{KM}^N and h_M coefficients, thus

$$C_{KM}^N(J_1 J_2 J_3 L_1 L'_1 L_2 L'_2 m) = E_{KM}^N(J_1 J_2 L_1 L'_1 m) h_M(J_2 J_3 L_2 L'_2)$$

where

$$E_{KM}^N = (-)^{L'_1 + N + 1} (2 - \delta_{N,0}) (2 - \delta_{L_1, L'_1}) (2J_1 + 1) (2J_2 + 1)^{\frac{1}{2}} (2L + 1)^{\frac{1}{2}} (2L' + 1)^{\frac{1}{2}} \langle L_1 \ 1 \ L'_1 \ -1 | KO \rangle \sum_K (-)^{J_1 - m} \langle J_1 \ -m | KO \rangle \langle K - N \ M \ N | KO \rangle F(J'_1) \quad (5)$$

and

$$h_M(J_2 J_3 L_2 L'_2) = (2J + 1)^{-\frac{1}{2}} (-)^{J_3 - J_2} (2 - \delta_{L_2, L'_2}) \bar{Z}_1(L_2 J_2 L'_2 J_2; J_3 M) \quad (6)$$

Expression (5) for E_{KM}^N depends only on parameters of the primary radiation while expression (6) for h_M depends only on parameters of the secondary radiation. One can write expression (3) as:

$$A_{KM}^N = \sum_m P(m)_{L_1, L_1'} \sum_{L_1, L_1'} \frac{\delta_1^{P_1}}{(1+\delta_1^2)} E_{KM}^N(J_1 J_2 L_1 L_1' m) \times \sum_{L_2, L_2'} (\delta_2^{P_2} / (1+\delta_2^2)) h_M(J_2 J_3 L_2 L_2') \quad (7)$$

From expressions (1) and (7) one can introduce two quantities:

$$G_{mM}(\delta_1, \theta_1, \theta_2, \phi) = \sum_{L_1, L_1'} (\delta_1^{P_1} / (1+\delta_1^2)) \sum_{KN} E_{KM}^N(J_1 J_2 L_1 L_1' m) Q_K Q_M X_{KM}^N(\theta_1, \theta_2, \phi) \quad (8)$$

and

$$H_M(J_2 J_3 \delta_2) = \sum_{L_2, L_2'} (\delta_2^{P_2} / (1+\delta_2^2)) h_M(J_2 J_3 L_2 L_2') \quad (9)$$

Thus one can write the triple correlation function in terms of the two parameters G_{mM} and H_M , thus:

$$W(\theta_1, \theta_2, \phi) = \sum_{nM} P(m) G_{mM}(\delta_1, \theta_1, \theta_2, \phi) H_M(\delta_2) \quad (10)$$

where

$$H_M(\delta_2) = [h_M(J_2 \ L_2 \ L_2 J_3) + \delta_2 h_M(J_2 \ L_2 \ L_2' J_3) + \delta_2^2 h_M(J_2' \ L_2' \ J_3)] / (1 + \delta_2^2)$$

The angular distribution of the primary gamma-ray is obtained by averaging the triple correlation formula over all directions of the secondary gamma-ray, i.e. over θ_2 and ϕ . When this is done all terms for which $M \neq 0$ vanish, this provides:

$$\begin{aligned} W(\theta_1) &= \sum_m P_m(J_1) G_{mM}(\delta_1, \theta_1) \\ &= \sum_m P_m(J_1) \sum_{L_1, L_1'} \sum_K (2K+1)^{\frac{1}{2}} \frac{\delta_1^{P_1}}{1+\delta_1^2} E_{KO}^O(J_1 L_1 L_1' J_2^m) \\ &\quad \times Q_K X_{KO}^O(\theta_1) \end{aligned} \quad (11)$$

APPENDIX "B"

SELECTION RULES FOR GAMMA RAY TRANSITIONS AND UNITS OF TRANSITION STRENGTHS

The particle capture by an atomic nucleus results in an excited state with an excitation energy more than the particle binding energy in the compound system. The formed state can decay in different ways governed by energetics and selection rules. Gamma-ray emission can compete with particle emission because it is usually exoergic, the amount of energy available being of the order of several MeV. As a consequence, radiative capture will be the dominant process when resonances occur for sufficiently low energies of the incident particle and when there are no competing exoergic reactions. When the incident particle is charged the widths for reemission are tremendously reduced by a coulomb barrier, so that radiative capture can be the dominant compound nuclear process over a considerable range in energy. However, if neutron emission (e.g. a (p,n) reaction) is possible it will generally be more probable than gamma-ray emission.

The probability of particle emission (72) is proportional to V/R , where V is the velocity of the particle and R is the nuclear dimension, while for gamma-

ray emission this probability is proportional to $e^2/\hbar C \cdot (V/C)^2$. V/R which is very small since $V/C < 1$ and $e^2/\hbar C$ is very small.

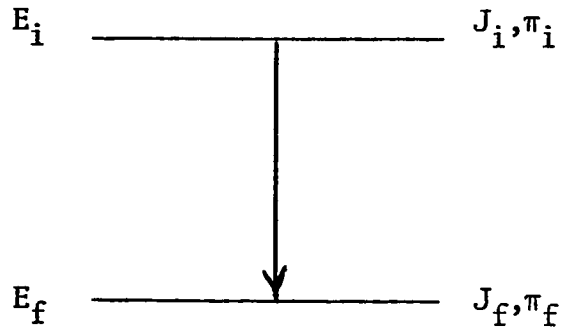


Figure 25 : Symbols for a gamma-ray transition.

B-1 Selection Rules

The general selection rules for an electromagnetic transition between an initial state of energy E_i , spin J_i and parity π_i and a final state E_f , spin J_f and parity π_f are summarized in the above Figure 25.

A) The energy of the emitted gamma-ray is given by:

$$E_\gamma = (E_i - E_f) / (1 + E_\gamma / 2MC^2)$$

where $E_\gamma / 2MC^2$ is the energy of the recoil nucleus and

is very small, hence $E_\gamma \approx E_i - E_f$.

- B) The angular momentum carried by the gamma quantum can have any of the values

$$|J_i - J_f| \leq L \leq J_i + J_f$$

- C) If J_i or $J_f = 0$; then only electric or only magnetic radiations could be emitted without any mixing.
- D) If $J_i = J_f = 0$; then the transition between these two sites by only one gamma quantum is forbidden. The transition between such states can go by means of a single electron (internal conversion) or through a pair emission if $E_i - E_f > 2m_0c^2$, these two processes can take place if parity does not change. If parity changes, then, this transition can occur by means of two internal conversion electrons or one internal conversion electron and one gamma quantum.
- E) The parity change between these two states as a result of gamma-ray emission is determined not only by the multipolarity L but also by the character of the transition whether electric or magnetic. The parity changes as $(-)^L$ for electric transitions and as $(-)^{L+1}$ for magnetic transitions. Table (7) lists multiplicities to be expected for a gamma-transition between

two states of specified angular momenta and parities.

TABLE 7
POSSIBLE MULTIPOLARITIES FOR GAMMA TRANSITION

Parity Change $\Delta\pi$	Change of Angular Momentum $ J_i - J_f $				
	0 or 1	2	3	4	5
No	M1(E2)	E2(M3)	M3(E4)	E4(M5)	M5(E6)
Yes	E1(M2)	M2(E3)	E3(M4)	M4(E5)	E5(M6)

Three further isospin selection rules are obtained when T is a good quantum number, viz.

- (i) all gamma-transitions are forbidden when $|\Delta T| > 1$
- (ii) E1 gamma-transitions are forbidden between two states in a self-conjugate nucleus (i.e., one with $N=Z$) when $\Delta T=0$.
- (iii) There may be an inhibitory effect on other multiples (e.g. on M2) when $\Delta T=0$.

Gamma-rays of different multipole orders and different characters can compete with each other in radiative transitions. The relative contribution of $L+1$ to L radiations (e.g. $M2$ to $E1$ or $E2$ to $M1$) is defined by Moskowski (73) as δ^2 and given by:

$$\delta^2 = \frac{\text{Intensity of radiation } L+1}{\text{Intensity of radiation } L} = \left(\frac{\langle J_f | L+1 | J_i \rangle}{\langle J_f | L | J_i \rangle} \right)^2$$

and definition of δ is taken to be $= \frac{\langle J_f \ L+1 \ J_i \rangle}{\langle J_f \ L \ J_i \rangle}$

The mixing ratio δ is real and can be either positive or negative depending on whether the two radiations are in phase or antiphase respectively. These relative contributions could be calculated according to the theory of electromagnetic transitions. The probability of transition by an electric radiation of multipolarity is given by:

$$T_E(L) = \frac{2\pi(L+1)}{L[(2L+1)!!]^2} \cdot \frac{K_{L+1}^2}{h} |Q_L|^2$$

The transition probability by a magnetic radiation of multipolarity L is given by:

$$T_M(L) = \frac{2\pi(L+1)}{L[(2L+1)!!]^2} \cdot \frac{K_{L+1}^2}{h} |M_L|^2$$

where $(2L+1)!! = 1 \times 3 \times 5 \dots 2L+1 = \frac{(2L+1)!}{2^L \times L!}$,

$K = \frac{1}{\lambda} =$ wave number of the gamma radiation,

Q_L , Q_M = electric and magnetic transitions when transforming from one state to another. The values of Q_L and M_L are proportional to the nuclear dimension as:

$$Q_L \sim R^L \quad \text{and} \quad M_L \sim V/C \cdot R^L$$

Hence:

$$T_E(L) \sim (R/\lambda)^{2L} \quad \text{and}$$

$$T_M(L) \sim (V/C)^2 (R/\lambda)^{2L}$$

Thus, the relative contributions of different radiations could be roughly estimated as:

$$T_M(L)/T_E(L) \sim (V/C)^2 \sim 10^{-2}$$

$$T_E(L)/T_E(L+1) \sim (R/\lambda)^{-2} \sim 10^{-4}$$

$$T_M(L)/T_E(L+1) \sim (V/C)^2 / (R/\lambda)^2 \sim 10^2$$

$$T_E(L)/T_M(L+1) \sim (R/\lambda)^{2L} / (V/C)^2 (R/\lambda)^{2L+2} \sim 10^6$$

$$T_E(L)/T_E(L+2) \sim (R/\lambda)^{2L} / (R/\lambda)^{2L+4} \sim 10^8$$

In the above calculations $V^2 = \frac{2E}{M} = 16 \times 10^{18} \text{ cm}^2/\text{sec}^2$,
 (E = kinetic energy of a nucleon of mass M in the nucleus
 and is of the order of the binding energy of the nucleon \sim
 8 MeV), $C = 3 \times 10^{10} \text{ cm/sec}$, $R = r_0 A^{1/3} \sim 1.3 \times 10^{-13} \text{ cm}$
 and $\lambda = \frac{Ch}{E} \sim 2 \times 10^{-11} \text{ cm}$ for a gamma-ray of energy 1 MeV.
 From these considerations we may arrive at the conclusion
 that in the analysis of experimental data we may neglect
 the contribution of higher order multipoles, e.g. we can
 neglect the contribution of M3 to E2 radiations.

B-2 Units of Transition Strengths

The transition probability of an excited nuclear
 state for gamma-radiation depends on the multipolarity, the
 energy of the gamma-ray and the wave functions of the
 nuclear states involved in the transition. Due to this
 dependence, significant information regarding nuclear wave
 functions can be obtained from a comparison of experimental
 gamma-decay transition probabilities with theoretical
 values (see reference 72) calculated on the basis of specific
 models of the nucleus. Hence, the most useful way to express
 the transition strength is in terms of a transition of the
 same energy and type calculated according to a certain
 model for a nucleus of the same size. The model most
 generally used is the extreme single particle model.

The results given for the strengths of radiative transitions for both electric 2^L -pole and magnetic 2^L -pole are measured in Weisskopf units.

For electric transitions if we measure " E_γ " in MeV and R in fermis we have:

$$\tau_Y^{-1}(\text{EL}) = \frac{4.4(L+1)}{L[(2L+1)!!]}^2 \cdot \left[\frac{3}{L+3} \right]^2 \cdot \left[\frac{E_\gamma}{197} \right]^{2L+1} \times R^{2L} \times 10^{21} \text{ sec}^{-1}$$

where $R = r_0 A^{1/3}$ and $r_0 = 1.20$ fermis. Then the radiative widths " Γ_γ " in ev for electric transitions are given in Weisskopf units as:

$$\Gamma_{\gamma W}(\text{E1}) = 6.8 \times 10^{-2} A^{2/3} E_\gamma^3 \text{ ev} ;$$

$$\Gamma_{\gamma W}(\text{E2}) = 4.9 \times 10^{-8} A^{4/3} E_\gamma^5 \text{ ev} ;$$

$$\Gamma_{\gamma W}(\text{E3}) = 2.3 \times 10^{-14} A^2 E_\gamma^7 \text{ ev} .$$

For magnetic transitions the calculation of the Weisskopf units are difficult because of the complication of the intrinsic magnetic moments of the nucleus. As was mentioned before, the magnetic matrix elements is smaller than the electric matrix element by a factor of the order V/C . This factor amounts to \hbar/MCR (see reference 72) where

"M" is the nucleon mass. Then the squares of the matrix elements for magnetic and electric transitions could be related by $10(\hbar/McR)^2$, which leads to:

$$\tau_Y^{-1}(\text{ML}) = \frac{1.9(L+1)}{L[(2L+1)!!]}^2 \cdot \left(\frac{3}{L+3} \right)^2 \left(\frac{E_Y}{197} \right)^{2L+1} \times R^{2L-2} \times 10^{21} \text{sec}^{-1}$$

and the Weisskopf estimates are:

$$\Gamma_{\gamma W}(\text{M1}) = 2.1 \times 10^{-2} E_Y^3 \text{ ev} ;$$

$$\Gamma_{\gamma W}(\text{M2}) = 1.5 \times 10^{-8} A^{2/3} E_Y^5 \text{ ev} ;$$

$$\Gamma_{\gamma W}(\text{M3}) = 6.8 \times 10^{-15} A^{4/3} E_Y^7 \text{ ev} .$$

APPENDIX "C"

75

GAMMA-RAY ANALYSIS PROGRAM

```

C
LOGICAL*1 STAR(4100,80),ST
DOUBLE PRECISION ACC(4100),ACCUM
CHARACTER*2 PQ(260),SQ(5),AQ(260),FQ(300)
CHARACTER*4 FIL,REC,EFFCOR
CHARACTER*1 DOT(101)
CHARACTER*8 SPIN(160)
DIMENSION CO(4100),E(4100)
REAL SLOPE,Y,A(128,2),ESET(2),X(4100,2),DL(10),
*LB,FEP(48),DEP(48),EM(48,3),CPK(260),UCPK(260),UPERC(260),
*PPE(260),DSE(260),EFSH(260),FULL(260),LEV(260),LLEVEL(260),
*FLEVEL(300),FCNTRD(300),FNTRD(300),FP(300),FRP(300),FPB(300),
*FUB(300),FPNET(300),FUPNET(300)
INTEGER CH(4100),MULTIP(4100),A1,A2,A3,A4,A5,A6,CSET(2),
*SC,RUN,Q(260),CAL,RITE,F(300)
*AT1,AT2,X1(260),X2(260),X3(260),X4(260),X5(260),X6(260),
*FX1(260),FX2(260),FX3(260),FX4(260),FX5(260),FX6(260)
DIMENSION ECNTRD(260),CNTRD(260),RP(260),T(50,2),
*URP(260),PB(260),PNET(260),UPNET(260),UB(260)
C.....
C.....
C.....
ISMTH=04
RUNSET=6
CALSET=0
RITE=1
EFFCOR='NO '
C.....
C.....
C.....
READ(8,1999)
IF(RITE.EQ.1)WRITE(9,1999)
1999 FORMAT (' ',/,/,/,/,/,/,/)
READ(8,*)RUN,CAL,FIL,REC,RESON,ERR
ERR=12.0
READ(8,*)AA,BB,CC
RUN=RUNSET
CAL=CALSET
IF(RITE.EQ.1)WRITE(9,75175)RUN,CAL,FIL,REC,RESON,ERR
IF(RITE.EQ.1.AND.CAL.EQ.0)WRITE(9,*)AA,BB,CC
75175 FORMAT(T2,2I6,1H',1H',A3,1H',1H',1H',A3,1H',2F8.1)
C$OPTIONS LINES=8400,WARN,NOLIST
READ(8,1099)
IF(RITE.EQ.1)WRITE(9,1099)
1099 FORMAT (' ')
C.....
C.....
C.....
DO 1119 IS=1,101
DOT(IS)='.'

```

DATA ST/'*'/

IF(RUN.LE.2)GO TO 3244

DATA FEP/0.94, 1.0, 1.05, 1.1, 1.17,1.25, 1.3, 1.38, 1.47,
 *1.52,1.6, 1.7, 1.8, 1.9, 2., 2.1, 2.22, 2.35 ,2.5 ,2.6 ,
 *2.75, 2.9 , 3.05 ,3.2 ,
 *3.35,3.55,3.7, 3.9 , 4.1 , 4.38, 4.6 , 4.8 , 5.1 , 5.4 ,5.8,
 *6.2, 6.5 ,6.9, 7.3, 7.8 , 8.4 , 8.9 , 9.6 , 10.5 ,11.5, 12.5,
 *13.5,15./

DATA DEP/ 2.25,2.35, 2.45, 2.55, 2.7, 2.8, 2.9 , 3. , 3.13
 *3.25, 3.37,3.5, 3.6 , 3.7 , 3.8 , 3.9 , 4., 4.05, 4.12, 4.2,
 *4.3, 4.35,4.4 ,4.405,4.41, 4.42, 4.43, 4.46, 4.48, 4.5 , 4.48
 *4.45 ,4.42,4.4, 4.37, 4.27 ,4.18, 4.03, 3.9 , 3.8 , 3.65 ,3.5,
 *3.3 , 3.1, 2.9 ,2.7 , 2.4 , 2.15/

EME=12000.

DO 324 JT=1,48

JE=48-JT+1

IF(JE.EQ.0)GO TO 324

EM(JE,1)=EME

EM(JE,2)=ALOG(FEP(JT))

EM(JE,3)=ALOG(DEP(JT))

EME=EME-200.

324 CONTINUE

CALL PLOT(22,EM,48,3,48,0,E,CO,DOT)

C
 C
 C
 C
 C .DEFINITIONS:
 C E=ENERGY
 C CH(X)=CHANNEL # X
 C CO(X)=COUNTS IN CHANNEL # X
 C ACC(X)=TOTAL COUNTS UP TO CHANNEL # X
 C
 C
 C

3244 EXECUTE HEAD

WRITE(6,66)

WRITE(6,77)

N=1

LOOP

IF(N.GT.410)QUIT

READ(8,7766)L\$, (DL(I4), I4=1,10)

ATEND,QUIT

IF(RITE.EQ.1)WRITE(9,7766)L\$, (DL(I4), I4=1,10)

N1=(N-1)*10

CO(N1+1)=DL(1)

CO(N1+2)=DL(2)

CO(N1+3)=DL(3)

CO(N1+4)=DL(4)

CO(N1+5)=DL(5)

CO(N1+6)=DL(6)

CO(N1+7)=DL(7)

CO(N1+8)=DL(8)

CO(N1+9)=DL(9)

CO(N1+10)=DL(10)

IF(RUN.EQ.0)WRITE(6,*)N1

IF(RUN.EQ.0)WRITE(6,1002)L\$, (CO(N1+I), I=1,10)

N=N+1

ENDLOOP

C

11221 CONTINUE

77

11 CONTINUE

EXECUTE HEAD

IF(IND.EQ.123456)EXECUTE LIMITN

IF(RUN.EQ.1)CALL PLOT(11,X,4100,2,4100,0,E,CO,DOT)

1002 FORMAT (/ ,T2,I5,10F8.0)

1333 FORMAT (T2,F8.2,2H| ,I4,2H| ,F11.1,2H| ,F8.1,2H| ,I3,2H| |)

44 FORMAT ('+',T48,80A1)

66 FORMAT ('1',T30,'FE56 (P,GAMMA) CO57')

77 FORMAT ('+',T30,'FE56 (P,GAMMA) CO57')

102 FORMAT (//T2,128(' '))

122 FORMAT (T2,128(' '))

3122 FORMAT ('+',T9,120(' '))

2122 FORMAT ('1',T47,A4,A4,/,T40,'THE UNCERTAINTY IS =',T62,F4.1)

1311 FORMAT(' ',T1,6I5,6X,2F9.1,2X,'R->',F7.1,4X,I3,A2,F9.1,3F11.2
*,1H%,5X,F6.3,/))

1211 FORMAT(T1,' PEAK # _____ PEAK LIMITS _____ CNTRD ECN
* TRANSITIN LINE RAW_COUNTS_CORR ERROR %ERR
* EFF. FACT.')

166 FORMAT ('+',50(' '))

103 FORMAT (T3,'|ENERGY|',T11,'CH.#',T16,'|ACCUM.COUNTS|',
CT33,'COUNTS|',T41,'|FACTOR|')

163 FORMAT (T3,'|ENERGY|',T11,'CH.#',T16,'|ACCUM.COUNTS|',
CT33,'COUNTS|',T41,'')

104 FORMAT (T3,'| KEV. |',T11,' ',T16,'|
CT33,' ',T41,'|X2**N |')

164 FORMAT (T3,'| KEV. |',T11,' ',T16,'|
CT33,' ',T41,'')

106 FORMAT (T2,1H| ,I3,A2,T10,1H| ,F8.1,T22,1H| ,F8.1,T33,1H| ,F12.1,
CT49,1H+,T48,F8.2,T59,1H| ,F12.1,T75,1H+,T74,F8.2,T86,1H| ,
CF12.1,T101,1H+,T100,F8.2,T115,1H| ,/'+',T49,1H_,T75,1H_,T101,1H
C/T2,128(' '))

206 FORMAT (T2,1H| ,I3,A2,T10,1H| ,F8.1,T22,1H| ,F8.1,T33,1H| ,F12.1,
CT49,1H+,T48,F8.2,T59,1H| ,F12.1,T75,1H+,T74,F8.2,T86,1H| ,
CF12.1,T101,1H+,T100,F8.2,T115,/'+',T49,1H_,T75,1H_,T101,1H_,
C/T2,128(' '),/,T60,'AFTER EFFICIENCY CORRECTION',T90,F9.1,
CT101,1H+,F8.1,T111,'OR',T114,1H+,F5.1,'%','+',T101,'-',
CT114,'-',/T2,128(' '))

107 FORMAT (1H ,1H| ,'PEAK#',T10,1H| ,' ENERGY ',T22,1H| ,' CENTROID'
C,T33,1H| ,' # OF COUNTS IN ROW PEAK ',T59,1H| ,'BACKGROUND UNDER

C' THE PEAK',T86,1H| ,'NET # OF COUNTS IN THE PEAK',T115,1H)

2222 FORMAT (T40,'THE # OF THE INTEGRATED PEAKS =',I4)

1222 FORMAT (1H)

323 FORMAT (//,6I10,//)

7533 FORMAT(/,' FROM',F8.1,' TO ',F8.1,A10,T40,A3,1H+,A3,1H+,A3,1H=
*T70,F9.0,T83,1H+,F8.0,/'+',T83,1H_,7X,' OR',T96,F6.2,'%','////

7333 FORMAT(/,' FROM',F8.1,' TO ',F8.1,A10,T40,A3,1H=
*T70,F9.0,T83,1H+,F8.0,/'+',T83,1H_,7X,' OR',T96,F6.2,'%','////

7433 FORMAT(/,' FROM',F8.1,' TO ',F8.1,A10,T40,A3,1H+,A3,1H=
*T70,F9.0,T83,1H+,F8.0,/'+',T83,1H_,7X,' OR',T96,F6.2,'%','////

7766 FORMAT(T5,I4,10(F7.0))

IF(RUN.EQ.1)EXECUTE PLOT

IF(RUN.EQ.2)EXECUTE PLOT

IF(RUN.LE.2)STOP

222 EXECUTE PEAK

STOP

C.....

C.....

C.....

C.....

C THE FOLLOWING BLOCK DOES THE FOLLOWING:

```

C .....
C .....
    IF(ISMTH.LT.1)GO TO 9211
    DO 7211 ISM=1,ISMTH
    CALL SMOOTH(CO,4100)
    PRINT,'CALL SMOOTH(CO,4100)'
7211 CONTINUE
9211 CONTINUE

C .....
C .....
C .....
    IF(RITE.NE.1)GO TO 3322
    DO 3321 NT=1,410
    L$=(NT-1)*10
    WRITE(9,7766)L$,(CO(L$+14),14=1,10)
    WRITE(6,*)L$
    WRITE(6,1002)L$,(CO(L$+1),1=1,10)
3321 CONTINUE
3322 CONTINUE

C .....
C .....
C .....
    READ(8,*)IND
    IF(RITE.EQ.1)WRITE(9,*)IND
    IF(IND.EQ.123456)EXECUTE LIMIT1
    IF(CAL.EQ.0)GO TO 756
    CALL CALIBR(AA,BB,CC,CO)
    IF(RITE.EQ.1)WRITE(9,*)AA,BB,CC
    GO TO 756
756 WRITE(6,*)'AA = ',AA,'BB = ',BB,'CC = ',CC
    IF(RUN.EQ.0)EXECUTE HEAD
    WRITE(6,122)
    WRITE(6,163)
    WRITE(6,164)
    WRITE(6,122)
    ACCUM=0.
    DO 11 I=1,4100
    CH(I)=I
    IF(RUN.GE.2)E(I)=AA*FLOAT(I**2)+BB*FLOAT(I)+CC
    IF(RUN.LE.1)E(I)=0.
    X(I,1)=I
    TEMP=CO(I)
    IF(TEMP.LE.0.0)TEMP=1.
    IF(CO(I).LE.0.0)CO(I)=1.
    X(I,2)=ALOG10(TEMP)
    ACCUM=ACCUM+CO(I)
    ACC(I)=ACCUM
    NSTAR=IFIX(CO(I))
    IF(NSTAR.EQ.0)NSTAR=1
    N=0
    MULTIP(I)=N
    IF(NSTAR.LE.80)GO TO 1007
1122 NSTAR=NSTAR/2
    MULTIP(I)=MULTIP(I)+1
    IF(NSTAR.GT.80)GO TO 1122
    NSTAR=80
1007 DO 515 K=1,NSTAR
    STAR(I,K)=ST
515 CONTINUE
    IF(NSTAR.GE.80)GO TO 11221

```

- .DEFINITIONS.....

NOP= # OF PEAKS

A6 = THE PEAK ATTRIBUTES

LB=AVERAGE BACKGROUND ON THE LEFT PER CHANNEL

RB=AVERAGE BACKGROUND ON THE RIGHT PER CHANNEL

RP(11)=RAW # OF COUNTS IN THE PEAK

AB=AVERAGE BACKGROUND

PB(11)=BACKGROUND COUNTS UNDER THE PEAK

PNET(11)=NET # OF COUNTS IN THE PEAK

UB(11)=UNCERTAINTY IN (PB(11))

URP(11)=UNCERTAINTY IN (RP(11))

UPNET(11)=UNCERTAINTY IN (PNÉT(11))

CNTRD(11)= CENTROID OF THE PEAK

ECNTRD(11)= ENERGY AT THE CENTROID

REMOTE BLOCK PEAK

EXECUTE HEAD

WRITE(6,122)

CALL LEVELS (LLEVEL, SPIN, NOL)

PRINT66

NOP=200

NU=200

IPC=0

DO 105 11=1,NOP

```
READ(8,*)S1,A3,A4,S2,FACTOR
```

ATEND, GO TO 1105

IF(S1.EQ.123456.)GO TO 1105

IF(A3.GT.0)GO TO 1411

IF(S1.LT.0.)GO TO 7519

A3=-A3

S1=1

A3=A3+1

IF(S2.LT.0.0)A3=A3-1

```
1411 IF(A4.GT.0)GO TO 1511
```

A4=-A4

S2=1

A4=A4-1

IF(S2.LT.0.0)A4=A4+1

1511 X1(I1)=S1

X2(I1)=A3

X3(11)=A4

X4(11)=S2

X5(11)=FA

$$X6(11)=A4-A3$$

IF(S1.LT.0.)C

SC=A3-10

DO 322 10

SC=SC+1

```

      T(IC,1)=SC
      T(IC,2)=CO(SC)
322  CONTINUE
7519 IF(RUN.LT.5)WRITE(6,2122)FIL,REC,ERR
      IF(RUN.GE.5)GO TO 3434
      WRITE(6,*)'
#,'
      THE SERIAL # OF THE PEAK---> ',I1
3434 CONTINUE
      IF(RUN.LT.5)WRITE(6,*)' '
      IF(RUN.LT.5)WRITE(6,*)S1,A3,A4,S2,FACTOR
      IF(RUN.LT.5)WRITE(6,*)'
      IF(S1.LT.0.)GO TO 7517
751  A1=A3-S1
      A2=A3-1
      A5=A4+1
      A6=A4+S2
      IF(RUN.LT.5)WRITE(6,*)' '
      IF(RUN.LT.5)WRITE(6,*)A1,A2,A3,A4,A5,A6
      IF(RUN.LT.5)WRITE(6,*)'
      IF(S1.EQ.0.)GO TO 752
      IF(S2.EQ.0.)GO TO 753
      GO TO 754
752  A1=A5
      A2=A6
      GO TO 754
753  A5=A1
      A6=A2
754  LB=(ACC(A2)-ACC(A1-1))/((A2-A1)+1)
CC   WRITE(6,*)LB,'LB'
      RB=(ACC(A6)-ACC(A5-1))/((A6-A5)+1)
CC   WRITE(6,*)RB,'RB'
      AB=(LB+RB)/2
CC   WRITE(6,*)AB,'AB'
      RP(I1)=(ACC(A4)-ACC(A3-1))
      RP(I1)=RP(I1)*ABS(FACTOR)
CC   WRITE(6,*)RP(I1),'RP'
      PB(I1)=AB*((A4-A3)+1)*ABS(FACTOR)
CC   WRITE(6,*)PB(I1),'PB'
      IF(FACTOR.EQ.2.0)PNET(I1)=RP(I1)-PB(I1)-0.5*(CO(A3)-AB)
      IF(FACTOR.EQ.-2.0)PNET(I1)=RP(I1)-PB(I1)-0.5*(CO(A4)-AB)
      IF(FACTOR.EQ.1.0)PNET(I1)=RP(I1)-PB(I1)
C    WRITE(6,*)PNET(I1),'PNET'
      UB(I1)=SQRT(PB(I1))
      URP(I1)=SQRT(RP(I1))
      UPNET(I1)=SQRT(RP(I1)+PB(I1))
      GO TO 7518
7517 S1=ABS(S1)
      A1=A2=A5=A6=0.
      RP(I1)=(ACC(A4)-ACC(A3-1))
      PB(I1)=S1*(A4-A3+1)
      AB=PB(I1)/((A4-A3)+1)
      PNET(I1)=RP(I1)-PB(I1)
      UB(I1)=SQRT(PB(I1))
      URP(I1)=SQRT(RP(I1))
      UPNET(I1)=SQRT(RP(I1)+PB(I1))
7518 SUMX=0.
      SUM=0.
      DO 155 I2=A3,A4
      SUMX=SUMX+(CO(I2)-AB)*FLOAT(I2)
      SUM=SUM+(CO(I2)-AB)

```

```

155 CONTINUE
    CNTRD(I1)=SUMX/SUM
    IF(FACTOR.EQ.-2.0)DEL=A4-CNTRD(I1)
    IF(FACTOR.EQ.-2.0)CNTRD(I1)=CNTRD(I1)+DEL
    IF(FACTOR.EQ. 2.0)DEL=CNTRD(I1)-A3
    IF(FACTOR.EQ. 2.0)CNTRD(I1)=CNTRD(I1)-DEL
    ECNTRD(I1)=AA*(CNTRD(I1)**2.)*BB*CNTRD(I1)+CC
C .....
C .....
C .....
C .....
    IF(RUN.LT.5)PRINT,' DO START'
    IFIND=0
    DO 5647 IS=1,NOL
    DIFF=ECNTRD(I1)-(RESON-LLEVEL(IS))
    IF(ABS(DIFF).LE.ERR)GO TO 5644
    IF(ECNTRD(I1).LT.1000.)GO TO 5643
    DIFF=DIFF+511.
    IF(ABS(DIFF).LE.ERR)GO TO 5645
    DIFF=DIFF+511.
    IF(ABS(DIFF).LE.ERR)GO TO 5646
    IF(IS.EQ.NOL.AND.IFIND.EQ.0)GO TO 5643
5660 GO TO 5647
C .....
C .....
C .....
5644 PQ(I1)='PP'
    IF(RUN.LT.5)PRINT,'DIFF= ',DIFF
    IF(RUN.LT.5)WRITE(6,*)' '
    IF(RUN.LT.5)WRITE(6,*)' '
    AQ(IS)=PQ(I1)
    Q(I1)=IS
    LEV(I1)=LLEVEL(IS)
    IF(RUN.LT.5)PRINT,IS,AQ(IS),LLEVEL(IS),'ASSS'
    IF(RUN.LT.5)WRITE(6,*)' '
    GO TO 5649
C .....
C .....
C .....
5645 PQ(I1)='SS'
    IF(RUN.LT.5)PRINT,'DIFF= ',DIFF
    AQ(IS)=PQ(I1)
    Q(I1)=IS
    LEV(I1)=LLEVEL(IS)
    IF(RUN.LT.5)PRINT,IS,AQ(IS),LLEVEL(IS),'ASSS'
    IF(RUN.LT.5)WRITE(6,*)' '
    GO TO 5649
C .....
C .....
C .....
5646 PQ(I1)='DS'
    IF(RUN.LT.5)PRINT,'DIFF= ',DIFF
    AQ(IS)=PQ(I1)
    Q(I1)=IS
    LEV(I1)=LLEVEL(IS)
    IF(RUN.LT.5)PRINT,IS,AQ(IS),LLEVEL(IS),'ASSS'
    IF(RUN.LT.5)WRITE(6,*)' '
C .....
C .....
C .....
5649 IPC=IPC+1

```

```

IFIND=IFIND+1
IF(RUN.LT.5)PRINT,'IFIND = ',IFIND
IF(RUN.LT.5)PRINT,'
IF(RUN.LT.5)PRINT,'IPC = ',IPC
IF(RUN.LT.5)PRINT,'
F(IPC)=IS
FQ(IPC)=AQ(IS)
FLEVEL(IPC)=LLEVEL(IS)
FCNTRD(IPC)=ECNTRD(I1)
FNTRD(IPC)=CNTRD(I1)
FP(IPC)=RP(I1)
FRP(IPC)=URP(I1)
FPB(IPC)=PB(I1)
FUB(IPC)=UB(I1)
FPNET(IPC)=PNET(I1)
FUPNET(IPC)=UPNET(I1)
FX1(IPC)=X1(I1)
FX2(IPC)=X2(I1)
FX3(IPC)=X3(I1)
FX4(IPC)=X4(I1)
FX5(IPC)=X5(I1)
FX6(IPC)=X6(I1)
IF(RUN.LT.5)WRITE(6,107)
IF(RUN.LT.5)WRITE(6,106)F(IPC),FQ(IPC),FCNTRD(IPC),FNTRD(IPC)
*,FP(IPC),FRP(IPC),FPB(IPC),FUB(IPC),FPNET(IPC),FUPNET(IPC)
IF(RUN.LT.5)PRINT,'
5647 CONTINUE
GO TO 3752
C .....
C .....
C .....
5643 IPC=IPC+1
IF(RUN.LT.5)PRINT,'IFIND = ',IFIND
IF(RUN.LT.5)PRINT,'
IF(RUN.LT.5)PRINT,'IPC = ',IPC
IF(RUN.LT.5)PRINT,'
PQ(I1)='UN'
IF(RUN.LT.5)PRINT,'DIFF= ',DIFF
IF(RUN.LT.5)PRINT,'
NU=NU+1
AQ(IS)=PQ(I1)
Q(I1)=NU
C PRINT,NU
LEV(I1)=-ECNTRD(I1)
IF(RUN.LT.5)PRINT,IS,AQ(IS),LLEVEL(IS),'ASSS'
IF(RUN.LT.5)WRITE(6,*)'
C .....
C .....
C .....
F(IPC)=NU
FQ(IPC)=AQ(IS)
FLEVEL(IPC)=LEV(I1)
FCNTRD(IPC)=ECNTRD(I1)
FNTRD(IPC)=CNTRD(I1)
FP(IPC)=RP(I1)
FRP(IPC)=URP(I1)
FPB(IPC)=PB(I1)
FUB(IPC)=UB(I1)
FPNET(IPC)=PNET(I1)
FUPNET(IPC)=UPNET(I1)

```



```

      FX1(IPC)=X1(I1)
      FX2(IPC)=X2(I1)
      FX3(IPC)=X3(I1)
      FX4(IPC)=X4(I1)
      FX5(IPC)=X5(I1)
      FX6(IPC)=X6(I1)
C .....
C .....
C .....
3752 IF(RUN.GE.5)GO TO 105
      WRITE(6,2122)FIL,REC,ERR
      WRITE(6,122 )
      WRITE(6,107)
      WRITE(6,122)
      WRITE(6,106)Q(I1),PQ(I1),ECNTRD(I1),CNTRD(I1),RP(I1),URP(I1),
*PB(I1),UB(I1),PNET(I1),UPNET(I1)
      WRITE(6,1222 )
      WRITE(6,122 )
      IF(RUN.LT.5)WRITE(6,103)
5117 IF(RUN.LT.5)WRITE(6,104)
      AT1=A3-10
      AT2=A4+10
      IF((AT2-AT1).GT.45)AT2=AT2-10
      JC=1
      DO 1555 IJ=AT1,AT2
C      WRITE(6,*)JC= ',JC
      T(JC,1)=IJ
      T(JC,2)=CO(IJ)
      JC=JC+1
      NSTAR=IFIX(CO(IJ))
      IF(NSTAR.EQ.0)NSTAR=1
      N=0
      MULTIP(IJ)=N
1111 IF(NSTAR.LT.80)GO TO 1000
      NSTAR=NSTAR/2
      MULTIP(IJ)=MULTIP(IJ)+1
      IF(NSTAR.GT.80)GO TO 1111
1000 DO 555 K=1,NSTAR
      STAR(IJ,K)=ST
      555 CONTINUE
      IF(RUN.LT.5)WRITE(6,1333)E(IJ),CH(IJ),ACC(IJ),CO(IJ),MULTIP(IJ)
      IF(RUN.LT.5)WRITE(6,44)(STAR(IJ,L),L=1,NSTAR)
      IF(RUN.LT.5)WRITE(6,166)
1555 CONTINUE
C      WRITE(6,323)A1,A2,A3,A4,A5,A6
C      WRITE(6,122)
C      WRITE(6,122)
C      WRITE(6,122)
      IF(RUN.LT.5)CALL PLOT(10,T,50,2,51,0,E,CO,DOT)
105 CONTINUE
1105 CONTINUE
      NOP=I1-1
      WRITE(6,2122)FIL,REC,ERR
      DO 800 I2=1,NOP
      WRITE(6,1321)I2,X1(I2),X2(I2),X3(I2),X4(I2),X5(I2),X6(I2)
800 CONTINUE
1321 FORMAT(T2,5G8.1,2G12.1,/)
      WRITE(6,2122)FIL,REC,ERR
      DO 3751 IR=1,IPC
      Q(IR)=F(IR)

```

```

PQ(IR)=FQ(IR)
LEV(IR)=FLEVEL(IR)
ECNTRD(IR)=FCNTRD(IR)
CNTRD(IR)=FNTRD(IR)
RP(IR)=FP(IR)
URP(IR)=FRP(IR)
PB(IR)=FPB(IR)
UB(IR)=FUB(IR)
PNET(IR)=FPNET(IR)
UPNET(IR)=FUPNET(IR)
X1(IR)=FX1(IR)
X2(IR)=FX2(IR)
X3(IR)=FX3(IR)
X4(IR)=FX4(IR)
X5(IR)=FX5(IR)
X6(IR)=FX6(IR)
IF(RUN.LT.5)WRITE(6,106)Q(IR),PQ(IR),ECNTRD(IR),CNTRD(IR),RP(I
*,URP(IR),PB(IR),UB(IR),PNET(IR),UPNET(IR)
3751 CONTINUE
IF(RITE.EQ.1)WRITE(9,*)NOP
WRITE(6,*)NOP
WRITE(6,*)' .....
WRITE(6,*)' .....
WRITE(6,*)' .....
WRITE(6,*)' .....
WRITE(6,*)' .....
WRITE(6,*)' .....
WRITE(6,*)' .....
WRITE(6,2222)NOP
WRITE(6,*)' .....
WRITE(6,*)' .....
WRITE(6,*)' .....
WRITE(6,*)' .....
WRITE(6,*)' .....
WRITE(6,*)' .....
CCCCCCCCCCCCCCCCCCCCCCCCCCCCCCCCCCCC OK
CCCCCCCCCCCCCCCCCCCCCCCCCCCCCCCCCCCC OK
CCCCCCCCCCCCCCCCCCCCCCCCCCCCCCCCCCCC OK
NOP=IPC
WRITE(6,2122)FIL,REC,ERR
PRINT,'          Q','          PQ','          LEV',
$          ECNTRD'
DO 2314 I7=1,NOP
WRITE(6,122)
PRINT,I7,Q(I7),PQ(I7),LEV(I7),ECNTRD(I7)
2314 CONTINUE
CCCCCCCCCCCCCCCCCCCCCCCCCCCCCCCCCCCC OK
CCCCCCCCCCCCCCCCCCCCCCCCCCCCCCCCCCCC OK
CCCCCCCCCCCCCCCCCCCCCCCCCCCCCCCCCCCC OK
DO 7123 IE=1,NOP
IF(RUN.LT.3)GO TO 7123
CC PRINT,'GOING TO EFFI'
EXECUTE EFFI
C WRITE(6,206)Q(IE),PQ(IE),ECNTRD(IE),CNTRD(IE),RP(IE),URP(IE),
C *PB(IE),UB(IE),PNET(IE),UPNET(IE),CPK(IE),UCPK(IE),UPERC(IE)
7123 CONTINUE
IF(RUN.GE.6)GO TO 2324
WRITE(6,2122)FIL,REC,ERR
PRINT,'          Q','          PQ','          LEV',
$          ECNTRD'

```

```

DO 1314 I7=1,NOP
WRITE(6,122)
IF(LEV(I7).LT.0.0)PRINT,I7,Q(I7),PQ(I7),LEV(I7),ECNTRD(I7)
1314 CONTINUE
2324 CONTINUE
CCCCCCCC OK
CCCCCCCC OK
CCCCCCCC OK
IF(RUN.LE.2)GO TO 8222
LINE=NOL
IF(RUN.GE.6)GO TO 8222
EXECUTE HEAD
WRITE(6,2122)FIL,REC,ERR
DO 7222 LN=1,300
NS=0
TOTC=0.
UT=0.0
DO 7111 IT=1,NOP
IF(Q(IT).NE.LN)GO TO 7111
WRITE(6,107 )
WRITE(6,122 )
WRITE(6,206)Q(IT),PQ(IT),ECNTRD(IT),CNTRD(IT),RP(IT),URP(IT),
*PB(IT),UB(IT),PNET(IT),UPNET(IT),CPK(IT),UCPK(IT),UPERC(IT)
TOTC=TOTC+CPK(IT)
IF(PQ(IT).EQ.'PP')GO TO 7331
IF(PQ(IT).EQ.'SS')GO TO 7331
IF(PQ(IT).EQ.'DS')GO TO 7331
CC
WRITE(6,1222)
WRITE(6,1222)
WRITE(6,*)'IF THE PEAK IS A PP'
WRITE(6,1222)
WRITE(6,*)'LOOK FOR THE FOLLOWING GAMMA RAYS:'
WRITE(6,1222)
EG1=ECNTRD(IT)-511.
EG2=EG1-511.
WRITE(6,1222)
WRITE(6,*)'SS ',EG1
WRITE(6,1222)
WRITE(6,*)'DS ',EG2
WRITE(6,1222)
WRITE(6,1222)
CC
CC
WRITE(6,*)'LOOK FOR THE FOLLOWING GAMMA RAYS:'
WRITE(6,*)'IF THE PEAK IS A SS'
WRITE(6,1222)
WRITE(6,*)'LOOK FOR THE FOLLOWING GAMMA RAYS:'
WRITE(6,1222)
EG0=ECNTRD(IT)+511.
EG2=EG0-511.-511
WRITE(6,1222)
WRITE(6,*)'PP ',EG0
WRITE(6,1222)
WRITE(6,*)'DS ',EG2
WRITE(6,1222)
WRITE(6,1222)
CC
WRITE(6,*)'IF THE PEAK IS A DS'
WRITE(6,1222)
WRITE(6,*)'LOOK FOR THE FOLLOWING GAMMA RAYS:'

```

```

WRITE(6,1222)
EG0=ECNTRD(IT)+511.+511.
EG1=EG0-511.
WRITE(6,1222)
WRITE(6,*)'PP ',EG0
WRITE(6,1222)
WRITE(6,*)'SS ',EG1
CC
CC WRITE(6,2122)FIL,REC,ERR
GO TO 7111
7331 NS=NS+1
SQ(NS)=PQ(IT)
UT=UT+UCPK(IT)**2
TRANS=LEV(IT)
7111 CONTINUE
UTOT=SQRT(UT)
IF(TOTC.EQ.0.)GO TO 7222
UREL=UTOT/TOTC*100
IF(NS.EQ.3)WRITE(6,7533)RESON,TRANS,SPIN(LN),SQ(1),SQ(2),SQ(3)
$,TOTC,UTOT,UREL
IF(NS.EQ.2)WRITE(6,7433)RESON,TRANS,SPIN(LN),SQ(1),SQ(2)
$,TOTC,UTOT,UREL
IF(NS.EQ.1)WRITE(6,7333)RESON,TRANS,SPIN(LN),SQ(1)
$,TOTC,UTOT,UREL
WRITE(6,122)
IF(NS.EQ.0)GO TO 7227
EG0=RESON-TRANS
EG1=EG0-511.
EG2=EG1-511.
WRITE(6,*)'THE EXPECTED GAMMA RAYS ARE:'
WRITE(6,1222)
WRITE(6,*)' PP SS
WRITE(6,1222)
WRITE(6,*)EG0,EG1,EG2
WRITE(6,1222)
7227 WRITE(6,2122)FIL,REC,ERR
7222 CONTINUE
8222 CONTINUE
WRITE(6,2122)FIL,REC,ERR
WRITE(6,1211)
DO 1124 IN=1,NOP
IF(IN.EQ.18)WRITE(6,2122)FIL,REC,ERR
IF(IN.EQ.36)WRITE(6,2122)FIL,REC,ERR
IF(IN.EQ.54)WRITE(6,2122)FIL,REC,ERR
IF(IN.EQ.72)WRITE(6,2122)FIL,REC,ERR
IF(IN.EQ.90)WRITE(6,2122)FIL,REC,ERR
IF(IN.EQ.108)WRITE(6,2122)FIL,REC,ERR
IF(IN.EQ.126)WRITE(6,2122)FIL,REC,ERR
IF(IN.EQ.144)WRITE(6,2122)FIL,REC,ERR
IF(IN.EQ.162)WRITE(6,2122)FIL,REC,ERR
IF(IN.EQ.180)WRITE(6,2122)FIL,REC,ERR
IF(IN.EQ.198)WRITE(6,2122)FIL,REC,ERR
IF(IN.EQ.216)WRITE(6,2122)FIL,REC,ERR
IF(IN.EQ.234)WRITE(6,2122)FIL,REC,ERR
IF(IN.EQ.252)WRITE(6,2122)FIL,REC,ERR
IF(IN.EQ.18)WRITE(6,1211)
IF(IN.EQ.36)WRITE(6,1211)
IF(IN.EQ.54)WRITE(6,1211)
IF(IN.EQ.72)WRITE(6,1211)
IF(IN.EQ.90)WRITE(6,1211)

```

```

IF(IN.EQ.108)WRITE(6,1211)
IF(IN.EQ.126)WRITE(6,1211)
IF(IN.EQ.144)WRITE(6,1211)
IF(IN.EQ.162)WRITE(6,1211)
IF(IN.EQ.180)WRITE(6,1211)
IF(IN.EQ.198)WRITE(6,1211)
IF(IN.EQ.216)WRITE(6,1211)
IF(IN.EQ.234)WRITE(6,1211)
IF(IN.EQ.252)WRITE(6,1211)
WRITE(6,122)
EFFM=CPK(IN)/PNET(IN)
WRITE(6,1311)IN,X1(IN),X2(IN),X3(IN),X4(IN),X5(IN),CNTRD(IN),
*ECNTRD(IN),LEV(IN),Q(IN),PQ(IN),PNET(IN),CPK(IN),UCPK(IN)
*,UPERC(IN),EFFM
IF(RITE.EQ.1)WRITE(9,75174)CNTRD(IN),ECNTRD(IN),LEV(IN),PQ(IN)
*Q(IN)
75174 FORMAT(T2,3F8.1,A2,I3)
IF(RITE.EQ.2)WRITE(81,*)ECNTRD(IN),CNTRD(IN),CPK(IN),UPERC(IN)
1124 CONTINUE
WRITE(6,2122)FIL,REC,ERR
END BLOCK
C*****
C*****
C*****
REMOTE BLOCK EFFI
CC PRINT,'Q ','PQ ','LEV ','ECNTRD'
CC PRINT,Q(IE),PQ(IE),LEV(IE),ECNTRD(IE)
C WRITE(6,*)PQ(IE),ECNTRD(IE),PNET(IE),UPNET(IE),'START E NET U
IF(PQ(IE).EQ.'SS')ECNTRD(IE)=ECNTRD(IE)+511.
IF(PQ(IE).EQ.'DS')ECNTRD(IE)=ECNTRD(IE)+2.*511.
IF(ECNTRD(IE).GT.12000.)GO TO 1761
IF(ECNTRD(IE).LT.2600.)GO TO 1761
IF(EFFCOR.EQ.'NO')GO TO 1761
RI=61.0-0.005*ECNTRD(IE)
C...RI=
CC WRITE(6,*)RI,'RI'
IRL=INT(RI)
CC WRITE(6,*)IRL,'IRL'
IRU=IRL+1
CC WRITE(6,*)IRU,'IRU'
RL=IRL
CC WRITE(6,*)RL,'RL'
DIF=RI-RL
CC WRITE(6,*)DIF,'DIF'
IF(PQ(IE).EQ.'SS')GO TO 325
IF(PQ(IE).EQ.'DS')GO TO 326
PPE(IE)=FEP(IRL)+DIF*(FEP(IRU)-FEP(IRL))
EFSH(IE)=PPE(IE)
CPK(IE)=PNET(IE)/PPE(IE)*100.
UCPK(IE)=UPNET(IE)/PNET(IE)*CPK(IE)
UPERC(IE)=UPNET(IE)/PNET(IE)*100.
CC WRITE(6,*)Q(IE),PQ(IE),PPE(IE),CPK(IE),UCPK(IE),UPERC(IE)
GO TO 327
326 DSE(IE)=DEP(IRL)+DIF*(DEP(IRU)-DEP(IRL))
EFSH(IE)=DSE(IE)
CPK(IE)=PNET(IE)/DSE(IE)*100.
UCPK(IE)=UPNET(IE)/PNET(IE)*CPK(IE)
UPERC(IE)=UPNET(IE)/PNET(IE)*100.
CC WRITE(6,*)Q(IE),PQ(IE),DSE(IE),CPK(IE),UCPK(IE),UPERC(IE)
GO TO 327

```



```
WRITE(6,*)'.....  
WRITE(6,*)'.....  
WRITE(6,*)'.....  
WRITE(6,*)'.....  
WRITE(6,*)'.....  
WRITE(6,*)'.....  
WRITE(6,*)'.....  
WRITE(6,122)  
WRITE(6,122)  
WRITE(6,122)  
WRITE(6,122 )  
WRITE(6,102 )  
WRITE(6,102)  
END BLOCK
```

END

SUBROUTINE PLOT

CALL PLOT (NO,A,N,M,NL,NS)

DESCRIPTION OF VARIOUS PARAMETERS:

NO - CHART NUMBER (3 DIGITS MAXIMUM)

A - MATRIX OF DATA TO BE PLOTTED. FIRST COLUMN REPRESENTS BASE VARIABLE AND SUCCESSIVE COLUMNS ARE THE CROSS-VARIABLES (MAXIMUM IS 9)

N - NUMBER OF ROWS IN MATRIX A (THERE IS NO LIMIT ON THIS)

M - NUMBER OF COLUMNS IN MATRIX A (EQUAL TO THE TOTAL NUMBER OF VARIABLES). MAXIMUM IS 10

NL - NUMBER OF LINES IN THE PLOT. IF 0 IS SPECIFIED, 50 LINES ARE USED(USUALLY TAKE $NL = N$ ----- BUT IN NO CASE $N > NL$; HOWEVER $N \leq NL$ CAN WORK. FOR $NL=0$, THE GRAPH IS CONFINED TO A SINGLE PAGE)

NS - CODE FOR SORTING THE BASE VARIABLE DATA IN ASCENDING ORDER

```
0  SORTING IS NOT NECESSARY (ALREADY IN ASCENDING
1  ORDER (0 OR ANY NEGATIVE INTEGER)
```

1 SORTING IS NECESSARY (1 OR ANY POSITIVE INTEGER)

SUBROUTINE PLOT(NO,A,N,M,NL,NS,E,CO,DOT)


```

DIMENSION OUT(101),YPR(11),ANG(9),A(1),E(4100),CO(4100)
CHARACTER*1 DOT(101)

```

```

C
C
C      THE CHARACTERS FOR THE GRAPHS CAN BE CHANGED ALSO -----
C
C      FOLLOWING DATA STATEMENT.
C

```

```

      DATA BLANK/' '/,ANG/'*','B','C','D','E','F','G','H',' '/
1  FORMAT(1H1,40X,'CHART # ',I3,T90,'----->>')
166 FORMAT ('+',T9,101A1)
2  FORMAT(1H ,F8.1,1X,1H|,100A1,2X,F8.1,1H|,F8.0)
3  FORMAT(1H )
7  FORMAT(1H ,16X,101H. . . . .)
@
177 FORMAT('+',15X,99('-'))

```

```

C
C
C      FORMAT STATMENT FOR Y-AXIS
C

```

```

8  FORMAT(1H ,9X,11F10.2)
   ITT=0
   NLL=NL

```

```

C
C
C      IF(NS) 16, 16, 10
C

```

```

C
C
C      SORT BASE VARIABLE IN ASCENDING ORDER
C

```

```

10 DO 15 I=1,N
   DO 14 J=1,N
   IF(A(I)-A(J)) 14, 14, 11
11  L=I-N
   LL=J-N
   DO 12 K=1,M
   L=L+N
   LL=LL+N
   F=A(L)
   A(L)=A(LL)
12  A(LL)=F
14  CONTINUE
15  CONTINUE

```

```

C
C
C      TEST NLL
C

```

```

16 IF(NLL) 20, 18, 20
18 NLL=50

```

```

C
C
C      WRITE TITLE
C

```

```

20 WRITE(6,1)NO

```

```

C
C
C      FIND SCALE FOR BASE VARIABLE
C

```

```

XSCAL=(A(N)-A(1))/(FLOAT(NLL-1))

```

```

C
C
C      FIND SCALE FOR CROSS-VARIABLES
C

```

```

M1=N+1
YMIN=A(M1)
YMAX=YMIN

```

```

      M2=M*N
      DO 40 J=M1,M2
      IF(A(J)-YMIN) 28,26,26
26  IF(A(J)-YMAX) 40,40,30
28  YMIN=A(J)
      GO TO 40
30  YMAX=A(J)
40  CONTINUE
      YSCAL=(YMAX-YMIN)/100.00
C
C      WRITE(6,*) CROSS-VARIABLE NUMBERS
C
      YPR(1)=YMIN
      DO 90 KN=1,9
90  YPR(KN+1)=YPR(KN)+YSCAL*10.0
      YPR(11)=YMAX
      WRITE(6,8)(YPR(IP),IP=1,11)
      WRITE(6,7)
C
C      FIND BASE VARIABLE PRINT POSITION
C
      XB=A(1)
      L=1
      MY=M-1
      I=1
45  F=I-1
      XPR=XB+F*XSCAL
      IF(A(L)-XPR) 50,50,70
C
C      FIND CROSS-VARIABLES
C
50  DO 55 IX=1,101
55  OUT(IX)=BLANK
      DO 60 J=1,MY
      LL=L+J*N
      JP=((A(LL)-YMIN)/YSCAL)+1.0
      OUT(JP)=ANG(J)
60  CONTINUE
C
C      FINDING AXIS FOR BASE VARIABLE.
C
      IF(YMIN.GT.0.)GO TO 100
      KP=1.-YMIN/YSCAL
      OUT(KP)=ANG(9)
C
C      PRINT LINE AND CLEAR, OR SKIP
C
100 ITT=IFIX(XPR)
      IF(ITT.GT.4100)ITT=1
      WRITE(6,2)XPR,(OUT(IZ),IZ=2,101),E(ITT),CO(ITT)
      WRITE(6,166)(DOT(ID),ID=1,JP)
C  WRITE(6,166)
      WRITE(6,177)
      L=L+1
      GO TO 80
70  WRITE(6,3)
80  I=I+1
      IF(I-NLL) 45, 84, 86
84  XPR=A(N)
      GO TO 50

```

[illegible]

```

C      WRITE(6,*) TITLE
C
C 20  WRITE(6,1)NO
C
C      FIND SCALE FOR BASE VARIABLE
C
C 20  XSCAL=(A(N)-A(1))/(FLOAT(NLL-1))
C
C      FIND SCALE FOR CROSS-VARIABLES
C
C      M1=N+1
C      YMIN=A(M1)
C      YMAX=YMIN
C      M2=M*N
C      DO 40 J=M1,M2
C        IF(A(J)-YMIN) 28,26,26
C 26  IF(A(J)-YMAX) 40,40,30
C 28  YMIN=A(J)
C      GO TO 40
C 30  YMAX=A(J)
C 40  CONTINUE
C      YSCAL=(YMAX-YMIN)/100.00
C
C      WRITE(6,*) CROSS-VARIABLE NUMBERS
C
C      YPR(1)=YMIN
C      DO 90 KN=1,9
C 90  YPR(KN+1)=YPR(KN)+YSCAL*10.0
C      YPR(11)=YMAX
C      WRITE(6,8)(YPR(IP),IP=1,11)
C      WRITE(6,7)
C
C      FIND BASE VARIABLE WRITE(6,*) POSITION
C
C      XB=A(1)
C      L=1
C      MY=M-1
C      I=1
C 45  F=I-1
C      XPR=XB+F*XSCAL
C      IF(A(L)-XPR) 50,50,70
C
C      FIND CROSS-VARIABLES
C
C 50  DO 55 IX=1,101
C 55  OUT(IX)=BLANK
C      DO 60 J=1,MY
C      LL=L+J*N
C      JP=((A(LL)-YMIN)/YSCAL)+1.0
C      OUT(JP)=ANG(J)
C 60  CONTINUE
C
C      FINDING AXIS FOR BASE VARIABLE.
C
C      IF(YMIN.GT.0.)GO TO 100
C      KP=1.-YMIN/YSCAL
C      OUT(KP)=ANG(9)
C
C      WRITE(6,*) LINE AND CLEAR, OR SKIP

```

```

100  ITT=IFIX(XPR)
C    WRITE(6,*)ITT
      WRITE(6,2)XPR,(OUT(IZ),IZ=2,101),E(ITT),CO(ITT)
      WRITE(6,166)(DOT(ID),ID=1,JP)
C    WRITE(6,166)
      L=L+1
      GO TO 80
70   WRITE(6,3)
80   I=I+1
      IF(I-NLL) 45, 84, 86
84   XPR=A(N)
      GO TO 50

C
C    WRITE(6,*) CROSS-VARIABLE NUMBERS AGAIN
C
C 86  WRITE(6,7)
C    WRITE(6,8)(YPR(IP),IP=1,11)
C
C
86  RETURN
    END
C*****
C*****
C*****
C*****
C*****
C CALIBR PROGRAM
  SUBROUTINE CALIBR (AA, BB, CC,CO )
C
  DIMENSION W(50) , F(3,50), U(50), P(4,4),Q(4,9),T1(4),
1 B(4), B1(4), NUM(4) ,CO(4100),SPEC (4100) , C(4)
  DIMENSION COEFF(3,20), TITLE(5,20), IANGL(20)
  LUNC = 5
  LUNT = 6
  LUNP = 7
1 NSPEC=1
  WRITE(6,*)NSPEC
  IF(NSPEC) 8000,8000, 8001
8000 WRITE(6,6003)
      CALL EXIT
8001 WRITE(6,6003)
      DO 6000 LSPEC = 1, NSPEC
        NFIRS=1
        NLAST=4100
        CHECK=2
        TMC=0
C      READ(8,*) NFIRS, NLAST, E1, E2, E3, E4, CHECK, TMC
C      WRITE(6,*)NFIRS, NLAST, E1, E2, E3, E4, CHECK, TMC
C      READ(8,*)IANGL(LSPEC), (TITLE(I,LSPEC), I = 1, 5)
C      WRITE(6,*)IANGL(LSPEC), (TITLE(I,LSPEC), I = 1, 5)
C      READ(8,*)( B1(I) , NUM(I) , I = 1 , 4 )
        READ(8,*)E1, B1(1) , NUM(1)
        READ(8,*)E2, B1(2) , NUM(2)
        READ(8,*)E3, B1(3) , NUM(3)
        READ(8,*)E4, B1(4) , NUM(4)
C      WRITE(6,*)( B1(I) , NUM(I) , I = 1 , 4 )
        IF(TMC) 5001, 5001, 5000
5000 DO 711 IM=1,NLAST
        SPEC(IM)=CO(IM)
711 CONTINUE

```

```

C5000 READ(8,*)(SPEC(I), I = 1, NLAST)
C    WRITE(6,*)(SPEC(I), I = 1, NLAST)
      GO TO 5002
5001 DO 722 IN=1,NLAST
      SPEC(IN)=CO(IN)
722 CONTINUE
C5001 READ(8,*)(SPEC(I), I = 1,NLAST)
C    WRITE(6,*)(SPEC(I), I = 1,NLAST)
      READ(8,*)LIMC
      IF(LIMC.EQ.123456)WRITE(6,*)'CALIBRATION DATA ENTERED'
      IF(LIMC.NE.123456)WRITE(6,*)'CHECK CALIBRATION DATA'
5002 IF (CHECK) 352, 352, 353
352 K2 = 3
      GO TO 355
353 K2 = 4
355 DO 14 K3 = 1, K2
      J = K3
      NPTS = NUM(J)
      M = B1(J)
      DO 3 K = 1, NPTS
        L = M+ K - 1
        WRITE(6,*)L
        U(K) = ALOG ( SPEC (L) )
3      W(K) = SPEC (L)
        DO 4 K = 1, NPTS
          F(1,K) = 1.0
          F(2,K) = K- 1
4        F(3,K) = F(2,K) *F(2,K )
          L$ = 3
          DO 12 J = 1,L$
            DO 12 I = J,L$
              P(I,J) = 0.0
              DO 11 K = 1,NPTS
11          P(I,J) = P(I,J) + W(K)*F(I,K)*F(J,K)
12          P(J,I) = P(I,J)
              DO 13 I = 1,L$
                B(I) = 0.0
                DO 13 L = 1,NPTS
13          B(I) = B(I) + W(L)*U(L)*F(I,L)
C    MATRIX INVERSION
      IF( L$ - 1 ) 307,307,49
307 B(1) = B(1)/ P(1,1)
      GO TO 306
49 M1 = 2*L$ + 1
      DO 3012 J = 1 , M1
        DO 3011 K = 1 , L$
3011 Q(K,J) = 0.
3012 CONTINUE
        DO 23 I = 1,L$
          DO 20 J = 1,L$
20          Q(I,J) = P(I,J)
23 CONTINUE
        DO 3013 I = 1,L$
          L = L$ + I
3013 Q(I,L) = 1.
          DO 59 I = 1,L$
59          Q(I,M1) = B(I)
          DO 68 J = 1,L$
            IF ( L$ - J ) 3004,3004,60
60 DO 61 I = J , L$

```

```

61 T1(I) = ABS ( Q(I,J) )
   M = J
   HOLE = T1(J)
   DO 63 I = J, L$
   IF ( HOLE - T1(I) ) 62, 63, 63
62 HOLE = T1(I)
   M = I
63 CONTINUE
   DO 64 K = J, M1
   BUMP1 = Q(J, K)
   Q(J, K) = Q(M, K)
64 Q(M, K) = BUMP1
3004 T1(J) = 1.0/Q(J, J)
   DO 65 K = J, M1
65 Q(J, K) = T1(J)*Q(J, K)
   Q(J, J) = 1.
   IF ( L$ - J ) 50, 50, 3005
3005 M = J + 1
   DO 67 N = M, L$
   BOX = Q(N, J)
   DO 66 K = J, M1
66 Q(N, K) = Q(N, K) - BOX*Q(J, K)
67 Q(N, J) = 0.
68 CONTINUE
50 DO 3010 J = 1, L$
   L = L$ + 1 - J
   N2 = L$ - J
   DO 3007 K = 1, N2
   BOX = Q(K, L)
   DO 3006 M = L, M1
3006 Q(K, M) = Q(K, M) - Q(L, M)*BOX
3007 CONTINUE
   IF ( L-2 ) 51, 51, 3010
3010 CONTINUE
51 DO 53 I = 1, L$
53 B(I) = Q(I, M1)
   DO 55 J = 1, L$
   DO 54 I = J, L$
   L = J + L$
   P(I, J) = Q(I, L)
54 P(J, I) = P(I, J)
55 CONTINUE
306 M = K3
   C(M) = -B(2) / (2.0*B(3) )
14 CONTINUE
   C1 = C(1) + B1(1)
   C2 = C(2) + B1(2)
   C3 = C(3) + B1(3)
   DENOM = C1*C1*(C2-C3)+C2*C2*(C3-C1)+C3*C3*(C1-C2)
   TOP1 = E1*(C2-C3)+E2*(C3-C1)+E3*(C1-C2)
   TOP2 = C1*C1*(E2-E3)+C2*C2*(E3-E1)+C3*C3*(E1-E2)
   X = TOP1/DENOM
   Y = TOP2/DENOM
   Z = E3 - X*C3*C3 - Y*C3 + Y/2.0
   IF ( CHECK ) 350, 350, 351
351 C4 = C(4) + B1(4)
   E5 = X*C4*C4 + Y*C4 + Z - Y/2.0
   WRITE(6, 205) E5, E4
350 COEFF(1, LSPEC) = X
   COEFF(2, LSPEC) = Y

```

```

      COEFF(3, LSPEC) = Z
      AA= COEFF(1, LSPEC)
      BB=COEFF(2, LSPEC)
      CC=COEFF(3, LSPEC)
      WRITE(6,*)AA,BB,CC
C     WRITE(6,204) IANGL(LSPEC), (TITLE(I, LSPEC), I = 1, 5)
      WRITE(6,203)(COEFF(I, LSPEC), I = 1, 3)
      WRITE(6,203) E1 , E2 , E3
      WRITE(6,203)C1 , C2 , C3
      WRITE(6,207)
      IF(LSPEC - 10) 6000,6004,6000
6004 WRITE(6,6003)
6000 CONTINUE
      DO 6002 LSPEC = 1, NSPEC
C     WRITE(6,204)IANGL(LSPEC), (TITLE(I, LSPEC), I = 1, 5)
6002 WRITE(6,203)(COEFF(I, LSPEC), I = 1, 3)
      203 FORMAT (3(3X, E13.6))
C 204 FORMAT (15, 5A4)
      205 FORMAT(20H TEST PEAK, FITTED =,F10.4, 9H ACTUAL =,F10.4 )
      207 FORMAT (/)
6003 FORMAT(1H1)
      RETURN
      END
C*****
C*****
C*****
C*****
C*****
      SUBROUTINE SMOOTH (Y,NPTS)
      DIMENSION Y(4100)
      11 IMAX=NPTS-1
      YI= Y(1)
      21 DO 24 I=1,IMAX
      YNEW=(YI+2.*Y(I)+Y(I+1))/ 4.0
      YI=Y(I)
      24 Y(I)=YNEW
      25 Y(NPTS)=(YI+3.*Y(NPTS)) /4.0
      RETURN
      END
C*****
C*****
C*****
C*****
C*****
      SUBROUTINE LEVELS(LLEVEL,SPIN,NOL)
C     PRINT,'ONE'
      REAL LLEVEL(160)
      CHARACTER*8 SPIN(160)
      NOL=1
      LOOP
C     PRINT,'TWO'
C     READ(9,*)LLEVEL(NOL),SPIN(NOL)
      READ,LLEVEL(NOL),SPIN(NOL)
      ATEND,QUIT
      WRITE(6,*)NOL,LLEVEL(NOL),SPIN(NOL)
      NOL=NOL+1
      ENDLOOP
      NOL=NOL-1
C     PRINT,'THREE'
      RETURN

```


END

C*****
C*****
C*****
\$ENTRY

REFERENCES

1. J. Chadwick, Nature, 129, 312 (1932)
2. J. Chadwick, Proc. Roz. Soc., A136, 692 (1936).
3. D. Iwanenko, Nature, 129, 798 (1932).
4. W.Z. Heisenberg, Physik, 77,1;ibid. 78, 156; ibid. 80, 587.
5. H.C. Urey, F.G. Brickwedde, and G.N. Murphy, Phys. Rev., 39, 164 (1932).
6. H.C. Urey, F.G. Brickwedde, and G.N. Murphy, Phys. Rev., 40, 1 (1932).
7. J.R. Oppenheimer, Phys. Rev., 35, 939 (1930).
8. P.A.M. Dirac, Proc. Roy. Soc. A133, 60 (1931).
9. C.D. Anderson, Phys. Rev., 48, 491 (1933).
10. E.Z. Fermi, Physik 88, 161 (1934).
11. J.D. Cockcroft, and Walton, E.T.S., Proc. Roy. Soc. A137, 229 (1932).
12. R.J. Van De Graaff, and Van Atta, Phys. Rev. 43, 149 (1933).
13. W.Z. Heisenberg, Phys. 77, 1 (1932).

14. M.A. Tuve, N. Hydenberg, and L.R. Hatstad, Phys. Rev. 43, 1055 (1933).
15. G. Breit, E.U. Condon and R.D. Present, Phys. Rev. 50, 825 (1936).
16. E. Wigner, Phys. Rev. 51, 106 (1937).
17. E. Wigner, Phys. Rev. 56, 519 (1939).
18. R.K. Adair, Phys. Rev. 87, 1041 (1952).
19. N.M. Kroll and L.L. Foldy, Phys. Rev. 88, 1177 (1952).
20. W.A. Fowler, L.A. Delsasso, and C.C. Lauritsen, Phys. Rev. 49, 561 (1936).
21. H. Bethe, Rev. Mod. PHYS. 8, 82 (1937).
22. V.L. Fitch and J. Rainwater, Phys. Rev. 92, 789 (1953).
23. L.M. Cooper, and E.M. Hanely, Phys. Rev. 92, 801(1953).
24. A.B. Brown, C.Y. Chao, W.A. Fowler, and C.C. Lauretsen, Phys. Rev. 7, 88 (1949).
25. J.D. Anderson and C. Wong, Phys. Rev. Lett. 7, 250 (1961).
26. J.D. Anderson, C. Wong and J.W. McClure, Phys. Rev. 126, 2170 (1962).
27. J.D. Anderson and C. Wong, Phys. Rev. Lett. 8, 442 (1962).

28. J.D. Anderson, Isobaric Spin in Nuclear Physics, J.D. Fox and D. Robson, Editors, Academic Press, N.Y. 1966.
29. J.D. Fox, C.F. Moore, D. Robson, Phys. Rev. Lett. 12, 198 (1964).
30. D. Robson, Phys. Rev. 137, B535 (1965).
31. A.M. Lane, Phys. Rev. Lett. 8, 171 (1962).
32. P. Goldhammer and L.W. Seagondollar (Editors), Second Symposium on the Structure of Low-Medium Mass Nuclei, Ohio (1966).
33. S. Maripuu, Nucl. Phys. A123, 357 (1969).
34. S. Maripuu, Nucl. Phys. A153, 183 (1970).
35. S. Maripuu, Phys. Lett. 31B, 181 (1970).
36. I. Foder, I. Szentpetery and J. Szucs, Phys. Lett. 32B, 689 (1970).
37. I. Szentpetery and J. Szucs, Phys. Rev. Lett. 28, 387 (1972).
38. M. Sharader, H.V. Klapdor, G. Bergdolt and A.M. Bergdolt, Phys. Lett. 60B, 39 (1975).
39. J.F. Matega, G.F. Neal, J.D. Goss, P.R. Chagnor and C.P. Brown, Phys. Rev. C13, 118 (1976).

40. L. Satpathy and S.C. Gojrahy, Nucl. Phys. A110, 400 (1968).
41. J.M.G. Gomes, Phys. Rev. C6, 149 (1972).
42. A. Corello and V.A. Manferdi, Phys. Lett. 34B, 584 (1971).
43. K.W.C. Stewart, B. Castel and B.P. Singh, Phys. Rev. C4, 2131 (1971).
44. R.L. Auble, Nucle. Data Sheets 20, 327 (1977).
45. C.M. Sedrer, S.S. Shirley (Editors), Table of Isotopes. John Wiley and Sons, Inc. N.Y. (1978).
46. S.E. Arnell and P.O. Persson, Arkiv Fysik 26, 193 (1964).
47. P.O. Persson and S.E. Arnell, Arkiv Fysik 33, 371 (1966).
48. B. Rosner and C.H. Holbrow, Phys. Rev. 145, 1080 (1967).
49. H. Brandle, W.R. Wylie, F. Zamboni and W. Zich, Nucl. Phys A151, 211 (1970).
50. B.J. O'Brien and G.E. Coote, Nucl. Phys. A153, 593 (1970).
51. J.R. Leslie, W. McLatchie, C.F. Monahan and J.K. Thrashev, Nucl. Phys. A170, 115 (1971).

52. D.P. Lindstorm, H.W. Newson, E.G. Bilpuch and G.E. Mitchell, Nucl. Phys. A168, 37 (1971).
53. G. Hardie, T.H. Braid, L. Meyer-Schutzmeister, and J.W. Smith, Phys. Rev. C5, 1600 (1972).
54. S. El-Kateb and G.M. Griffiths, Nucl. Phys. A240, (1975) 120.
55. S. El-Kateb and G.M. Griffiths Z. Phys A30 (1981) 189.
56. Foder, J. Sziklai, B. Kardon, J. Rama Rao, K. Beckert, F. Hermann and H. Schobber, J. Phys 64, 1117 (1978).
57. C. Rangacharyalu, I.M. Szoghy, C. St. Pierr and K. Ramarataram, Phys Rev C19, 1762 (1979).
58. W.A. Watson III, E.G. Bilpuch and G.E. Mitchell, Phys. Rev. C24, 1992 (1982).
59. E. Arai, M. Futakutchi, H. Kamada, J. Komaki, T. Matsusaki, M. Ogawa and Y. Oguri, Nucl Phys A378 (1982) 259.
60. J.B. Marion and F.C. Young, Nuclear Reaction Analysis, Wiley and Sons (1968).
61. R.J. De Meijer, H.S. Blendl and R. Holub, Atomic Data Tables 13,1 (1974).
62. G.I. Harris, H.J. Hennecke and D.D. Watson, Phys Rev, B139,1113 (1965).

63. A.K. Hyder and D.D. Watson, Aerospace Research Laboratory Report, ARL67-0168 (1967).
64. G.U. Din, Nucl. Phys. A134, 655 (1969).
65. A. Adam, O. Bersillon and S. Joly, Phys. Rev. C14, 92 (1976).
66. M.M. Nagadi, "Search for the $g_{9/2}$ Analogue State in ^{59}Co Via The $^{58}\text{Fe} (P, \gamma) ^{59}\text{Co}$ Reaction", M.Sc. Thesis, University of Petroleum and Minerals, Dhahran, Saudi Arabia (1984).
67. A.J. Ferguson and A.R. Rutledge, Atomic Energy Canada, Ltd. CRP-615, AECL-420, 1962 (unpublished).
68. P.B. Smith, Nuclear Reaction, edited by P.M. Endt and P.B. Smith (North Holland Publishing Company, Amsterdam, 1962), Vol. II.
69. P.B. Smith, Can. J. Phys. 42, 1101 (1964).
70. A.J. Ferguson, Angular Correlation Methods in Gamma-Ray Spectroscopy (North Holland Publishing Company, Amsterdam, 1965).
71. R.D. Gill, Gamma-Ray Angular Correlation (Academic Press, London, New York, San Francisco 1975).
72. D.H. Wilkinson, Nuclear Spectroscopy Part B, ed. F. Ajzenberg-Selove, Academic Press, N.Y. (1960).
73. S.A. Moskowski "Beta and Gamma-Ray Spectroscopy", ed., K. Siegbahn, North Holland Amsterdam (1955)